



# Using visible light to activate antiviral and antimicrobial properties of TiO<sub>2</sub> nanoparticles in paints and coatings: focus on new developments for frequent-touch surfaces in hospitals

M. Schutte-Smith, E. Erasmus , R. Mogale, N. Marogoa, A. Jayiya, H. G. Visser

Received: 27 July 2022 / Revised: 27 October 2022 / Accepted: 30 October 2022  
© American Coatings Association 2023

**Abstract** The COVID-19 pandemic refocused scientists the world over to produce technologies that will be able to prevent the spread of such diseases in the future. One area that deservedly receives much attention is the disinfection of health facilities like hospitals, public areas like bathrooms and train stations, and cleaning areas in the food industry. Microorganisms and viruses can attach to and survive on surfaces for a long time in most cases, increasing the risk for infection. One of the most attractive disinfection methods is paints and coatings containing nanoparticles that act as photocatalysts. Of these, titanium dioxide is appealing due to its low cost and photoreactivity. However, on its own, it can only be activated under high-energy UV light due to the high band gap and fast recombination of photogenerated species. The ideal material or coating should be activated under artificial light conditions to impact indoor areas, especially considering wall paints or frequent-touch areas like door handles and elevator buttons. By introducing dopants to TiO<sub>2</sub> NPs, the bandgap can be lowered to a state of visible-light photocatalysis occurring. Naturally, many researchers are exploring this property now. This review article highlights the most recent advancements and research on visible-light activation of TiO<sub>2</sub>-doped NPs in coatings and paints. The progress in fighting air pollution and personal protective equipment is also briefly discussed.

## Graphical Abstract

M. Schutte-Smith, E. Erasmus (✉), R. Mogale, N. Marogoa, A. Jayiya, H. G. Visser (✉)  
Department of Chemistry, University of the Free State, P.O. Box 339, Bloemfontein 9300, South Africa  
e-mail: erasmuse@ufs.ac.za

H. G. Visser  
e-mail: visserhg@ufs.ac.za

Indoor visible-light photocatalytic activation of reactive oxygen species (ROS) over TiO<sub>2</sub> nanoparticles in paint to kill bacteria and coat frequently touched surfaces in the medical and food industries.



**Keywords** TiO<sub>2</sub>, Photocatalysis, Antibacterial, Coating, Visible-light activation

## Introduction

Nosocomial infections account for 7% of hospitalizations in developed countries and 10% in undeveloped countries. Bacteria like *Pseudomonas aeruginosa* can survive on inanimate surfaces for days to months and *Candida albicans* from 1 to 120 days.<sup>1–3</sup> Viruses mostly do not last that long, with survival times ranging from a few hours to a few weeks. These pathogenic microorganisms and viruses (MoVs)<sup>4–6</sup> may cause life-threatening infections when entering the body through wounds, surfaces, or devices like catheters and intravenous lines. Furthermore, they can be self-transferred

by patients from their own hands to the mucosa of the mouth or nose. MoVs can be transported in three main ways: aerosolized, for example, through flushing toilets;<sup>7, 8</sup> kinematic, for example, an infected hand touching a surface,<sup>5</sup> and hydrodynamic, for example, the practice of dowsing certain vegetables in water and then freezing it to keep them crisp has been known to introduce waterborne bacteria to food.<sup>9</sup>

Healthcare-associated infections (HAIs) are connected to environmental surfaces, potential reservoirs for pathogens allowing transmission from surfaces to patients and vice versa. Polymicrobial biofilms are a densely packed community of organisms (fungi, bacteria, and viruses) that exist at a phase or density interface. They are embedded within an extracellular matrix, often consisting of polysaccharides.<sup>10</sup> In the human body, they shield the pathogenic microorganisms from antibodies and immune cells, resulting in chronic infections that are difficult to eliminate.<sup>11</sup> They can also be found on medical implants and inanimate surfaces, including food processing surfaces, walls, ceramics, steel, etc. To compound the apparent threat of these biofilms, they are known to enhance the production of biofilm masses of other species. They can have an adverse effect on disinfection and cleaning practices.<sup>12–15</sup> Biofilms do not only grow on wet surfaces; they can also be found in intensive care units and other surfaces in hospitals, as was shown by several research groups in the past.<sup>16–19</sup>

From the above, it is evident that there is a need for some form of surface protection or improvement to prevent microorganisms from attaching to them. However, the development of antimicrobial, antiviral surface coatings must consider that fungi, bacteria, and viruses interact differently with a surface. This is discussed in detail in the review of Tolker-Nielsen.<sup>20</sup>

The adherence of bacteria, for example, will be assisted by hydrophobic flagella. Very soon after the initial contact, the attachment can become gradually stronger within minutes by developing strategies to remove the obstructive water on the inanimate surface (see Fig. 1 for the steps followed during biofilm formation).<sup>21, 22</sup>

For the attachment of fungi to surfaces, hydrophobicity also plays a role. For example, *Candida albi-*

*cans* cells may alter the features of their cell wall to attach efficiently to surfaces with different physical or chemical properties and even change their surface feature from hydrophobic to hydrophilic depending on the temperature they find themselves in.<sup>23</sup>

The persistence of viruses on surfaces is affected by the material's porosity, humidity, temperature, light conditions, the presence of biofilms, and pH.<sup>24</sup> The potential of viral spreading via contaminated surfaces depends mainly on the total amount of virus deposited and the ability of the virus to maintain infectivity while it is in the environment. Attachments are primarily driven by electrostatic forces between ionizable amino acids or negative charges in the capsid.<sup>25</sup>

Limiting the continuous growth of pathogens on surfaces reduces the risk of transmission. Disinfection of surfaces is a big business. It is estimated that the global antimicrobial market size is more than USD 8 billion and will reach more than USD 20 billion by 2028.<sup>26</sup>

Although antimicrobial resistance is a natural phenomenon,<sup>27</sup> modern malpractice accelerated it. The cost to healthcare systems due to resistance is a serious problem worldwide. In 2016, a United Nations Bulletin estimated that antimicrobial resistance is directly responsible for more than 700 000 deaths annually.<sup>28</sup> The threat is not only related to microorganisms. The recent SARS-COVID-19 pandemic is an indication of that. Recent research has shown that the virus can survive for 28 days at 20°C on glass, stainless steel, and banknotes.<sup>29</sup>

Kumaravel et al.<sup>30</sup> mentioned in a recent review that antimicrobial coatings with innovative, environmentally responsive, multifunctional features, such as continuous antimicrobial protection with scratch, abrasion, chemical and stain resistance with easy cleaning properties, offer opportunities to fight microbial resistance and provide better protection against viral outbreaks. Accordingly, the manufacturing sector urgently needs visible-light-activated antimicrobial coatings that do not contain expensive additives like Ag. This is driven by the highest regulatory standards in health care, the food industry, construction, electronics, med-tech, pharma, public infrastructure, and home environments.

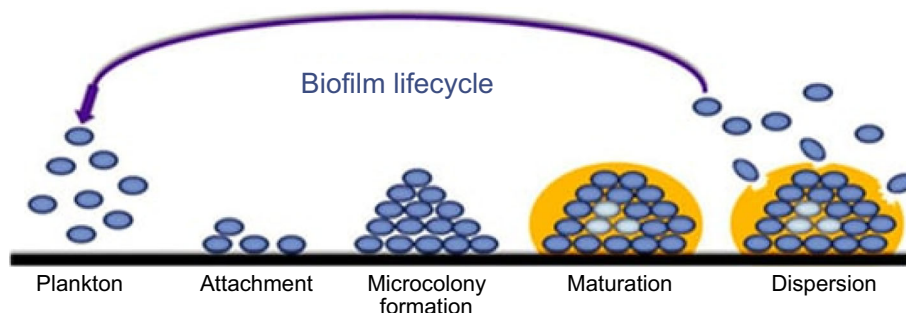


Fig. 1: Schematic representation of the steps followed during biofilm formation. Reprinted from: Achinas, S. et al. A brief recap of microbial adhesion and biofilms. *Appl. Sci.* 2019, 9, 2801,<sup>21</sup> with permission from MDPI

Wang et al.<sup>31</sup> recently reviewed the literature on commercial coatings for uses in spacecraft and space stations. The growth of biofilms in spacecraft is extenuated by the higher CO<sub>2</sub> concentrations, micro-gravity conditions, and high humidity. To complicate matters, the resistance of biofilms increases as the number of microorganisms in the film increases. This forces the use of combined antimicrobial strategies using different types of agents. Naturally, photocatalytic paints and coatings that generate ROS in visible-light conditions could be excellent foils to bacterium resistance.

Sun and co-workers discussed the lessons learned from the COVID-19 pandemic in terms of antiviral surfaces in a recent review article<sup>32</sup> and concluded that surfaces that provide antiviral ability through an excitonic effect to generate localized heat, light, free radicals, and free charges and carriers to kill or interfere with the adhesion and replication of the viruses and germs are probably one of the best and cheapest methods to combat future virus pandemics (see Fig. 2 for an illustration of promising antiviral coatings). Talebian et al.<sup>24</sup> proposed that future technologies should focus on disinfection using metal oxide NPs because of their inherent broad range of antiviral activities, persistence, and efficacy at low dosages.

They went a step further to suggest that the detection of the virus via nanotechnology could facilitate faster and more accurate identification even at the early stages of the infection due to the versatility of surface modification of nanoparticles.

Very shortly after the onset of the COVID-19 pandemic, NanoTechSurface, Italy, fabricated a robust and self-cleaning formula comprised of titanium dioxide and silver ions for disinfecting surfaces.<sup>33</sup> Similarly, FN Nano Inc., USA, developed a photocatalytic paint based on titanium dioxide nanoparticles,<sup>24</sup> which can destroy organic compounds like viruses on the surface upon exposure to light, damaging the viral membrane.

Recently, TiO<sub>2</sub> nanoparticles were shown effective against HCoV-NL63 under various humidity conditions. Khaiboullina et al.<sup>34</sup> showed that TiO<sub>2</sub> nanoparticles retain virucidal efficacy even at very high humid conditions (85% relative humidity), predicating for broader use of TiO<sub>2</sub> NPs coatings on outdoor surfaces. They illustrated that TiO<sub>2</sub>-coated surfaces have a viral inactivation property even on dried virus droplets.

Much research is being conducted to develop antimicrobial and antiviral coatings or paints for near-patient surfaces in hospitals and for applications in the food industry. Most of this research is focused on using various nanomaterials or combinations of them

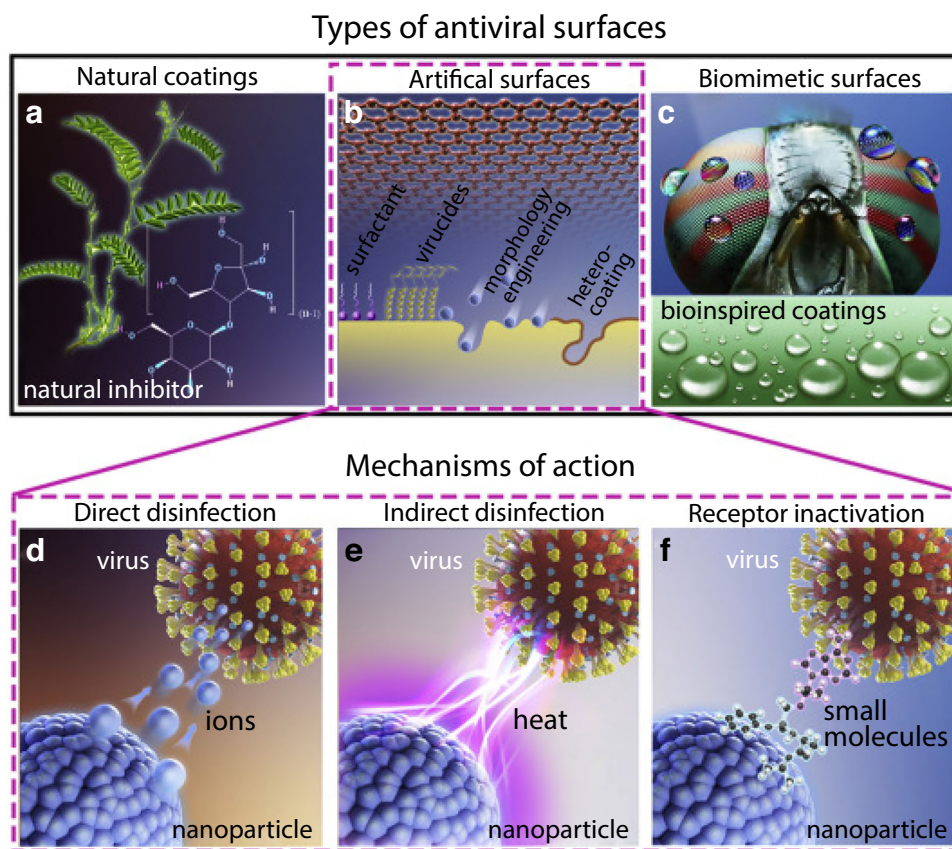


**Fig. 2: Promising antiviral coatings based on the selection of materials and engineering of surface nanostructures and the antiviral action mechanisms.** Reprinted from: Sun, Z. et al. Future antiviral surfaces: Lessons from COVID-19 pandemic. *Sustain. Mater. Technol.* 2020, 25, e00203,<sup>32</sup> (copyright 2020) with permission from Elsevier

with metals or polymers. Of these materials,  $\text{TiO}_2$  is perhaps the most well known. It is a photocatalyst that exists in three main crystallographic forms, namely anatase, brookite, and rutile. The bandgap of these forms varies between 3 and 3.2 eV rendering it ultraviolet-active but inactive in the visible-light region.<sup>35</sup> The disinfection nature of titania is well established to be about three times more effective than chlorine and 1.5 times more than ozone.<sup>36</sup> It can kill a wide range of bacteria, fungi, and viruses.<sup>37, 38</sup>

When exposed to ultraviolet light, it breaks down water vapor in the air to produce free oxygen radicals that will attack whatever is on the surface, including organisms like those mentioned before (see Fig. 3 for the proposed mechanism).<sup>39</sup> A recent review article discusses the mechanisms of disinfection using  $\text{TiO}_2$  in detail.<sup>40</sup> In short,  $\text{TiO}_2$  activates valence band electrons ( $e^-$ ) which move to the conduction band, generating an exciton pair and leaving a positively charged hole ( $h^+$ ) in the valence band. The  $e^-$  and  $h^+$  can recombine and either undergo recombination to radiatively or non-radiatively dissipate the excess energy as heat or light. This process can happen in the bulk of the NP or on the surface. The excitons can move to the surface and produce reactive oxygen species (ROS) by reacting with oxygen. The oxygen radicals formed can further react with  $\text{H}_2\text{O}$  to produce hydroxide radicals. The biocidal action of  $\text{TiO}_2$  materials is thus ascribed to ROS, which breaks down the cell membrane of biomatter, leading to lipid peroxidation<sup>41–44</sup> and eventually interfering with cellular respiration, inactivating a wide range of organisms.

There are several reasons why  $\text{TiO}_2$  NPs are so sought after. They have high photoreactivity, are inexpensive, are very stable chemically, and have a self-cleaning ability which prevents the formation of biofilm masses on the surface.<sup>45, 46</sup> They do have drawbacks too. Their fast electron–hole recombination, which corresponds to the degradation of the

photoelectric energy into heat, meaningfully restricts the photooxidation rate of biomaterials or organic compounds on the surface.<sup>47, 48</sup> To overcome this,  $\text{TiO}_2$  has been used with metal ions, noble metals, non-metals, other metal oxides, and polymeric structures like  $g\text{-C}_3\text{N}_4$ ,<sup>49–52</sup> to name a few, with improved results.

Due to the abovementioned, it is evident that there are opportunities to use  $\text{TiO}_2$  NPs in the healthcare environment, and unsurprisingly, they are considered by many researchers. There are many examples in the literature, ranging from applications where  $\text{TiO}_2$  was coated onto suture material for wound healing, on titanium implants, combined with nanofibers loaded with antibiotics as a controlled drug delivery system, used for self-sterilizing catheter coatings, on stainless steel as coatings and as paint additives or surface coatings.<sup>53–61</sup>

The physicochemical characteristics of NPs play a significant role in their efficacy against pathogenic microorganisms. Small-sized NPs boost antimicrobial and antibacterial properties due to the increase in the surface area-to-volume ratio; on the contrary, smaller particles are more toxic to mammalian cells, so increased leaching needs to be considered.<sup>62</sup>

The surface vacancy of NPs also plays a decisive role in biological activity. For example, the oxygen vacancy in  $\text{ZnO}$  NPs could be fine-tuned by doping on the Zn and O site by aliovalent substitution using, for example, N.<sup>63</sup> This resulted in an increased generation of ROS. This was also seen for  $\text{MoS}_2$  nanosheets, where an increase in nanoholes led to increased antibacterial activity. Unlike known antibacterial mechanisms, these nanoholes serve as electron donors to biofilms, leading to increased electron transport capacity and effectively destroying proteins, intercellular adhered polysaccharides, and extracellular DNA.<sup>63, 64</sup>

The surface morphology and crystallographic planes of NPs have importance in their all-over function. For example, spherical Ag nanoparticles were more effec-

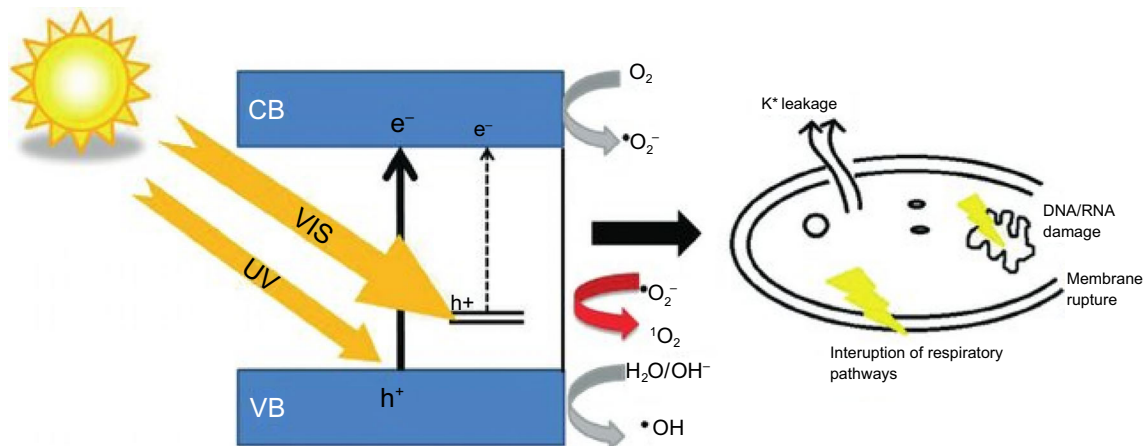


**Fig. 3: Schematic representation of the mechanism followed by  $\text{TiO}_2$  for bacterial disinfection using either UV or visible light. Reprinted from Fisher, M.B. et al., Nitrogen and copper doped solar light active  $\text{TiO}_2$  photocatalysts for water decontamination, *Appl. Catal. B*, 2013, 130–131, 8–13.<sup>39</sup> Copyright (2013), with permission from Elsevier**

tive against *Klebsiella pneumoniae* than rod-shaped silver NPs. Similarly, Ag nanoplates which formed a (111) lattice plane, exhibited the most potent bactericidal effect on *E. coli*.<sup>65</sup> Additionally, it was shown that the antibacterial activity of Cu<sub>2</sub>O nanocrystals is also facet dependent, with the octahedron morphology (exposing the (111) facet) displaying a higher antibacterial activity than the cubic morphology (exposing only the (100) facet).<sup>66</sup>

Several strategies prevent microorganisms from remaining on surfaces or destroying them. These include the self-explanatory kill-on-contact approaches, the release of antimicrobial substances by the coating over time, surfaces with high hydrophobicity or hydrophilicity, nanoprotusions, and/or combinations of two or more of these methods,<sup>26</sup> as discussed in detail in a recent review by Birkett et al. which covered many different types of nanomaterials and their antimicrobial applications.

Antifungal and antibacterial surfaces use similar destruction mechanisms, namely the generation of ROS and toxic ions. Antiviral actions of surfaces are categorized into six basic types.<sup>67</sup> Ionic surfaces such as metals and polyethylenimines degrade the RNA/DNA, photosensitizing materials producing ROS (such as TiO<sub>2</sub>),<sup>68</sup> adsorbing surfaces which cause membrane disruption through dehydration, sharp nanostructured surfaces like graphene cause membrane rupture through puncturing, controlled release of virucides by hydrogels and inactivating surfaces that contain biopolymers which can bind to the membrane or capsid protein.<sup>67</sup>

The recent review by Chen et al. discussed the incorporation strategies of TiO<sub>2</sub> and other nanoparticles in paint and how inorganic binders can prevent the photodegradation of organic binders or other molecules in the paint.<sup>69</sup> They also addressed the old argument about which of hydrophobic or hydrophilic surfaces are most efficient. On the one hand, hydrophobic surfaces could prevent biofouling or fungi and bacterial attachment. Conversely, hydrophilic surfaces promote better contact with biomatter and have improved moisture trapping essential for generating ROS.

Coatings that can improve the air quality in buildings in visible light have also been employed. In one such example, tungsten-doped TiO<sub>2</sub> nanoparticles incorporated into a coating for medium-density fiberboards showed higher activity in NO<sub>x</sub> degradation than commercial products.<sup>70</sup>

Over the years, the development of paints moved toward using waterborne formulations instead of traditional organic solvent-borne options. These are safer for the environment and have less odor. Waterborne paints typically contain additives, binders, dyes, fillers, pigments, plasticizers, and solvents. The addition of TiO<sub>2</sub> NPs to paints is not without challenges. The NPs can photodegrade the organic binders in the paint, and in some cases, the binders can trap NPs so that ROS cannot be generated.<sup>71</sup> There is a lot to consider in

coatings design; hydrophilicity versus hydrophobicity, washability, efficacy, leaching, and durability are just a few. Of these factors, durability is possibly the most important, as it has a direct financial impact. For example, when a coating of anatase/rutile TiO<sub>2</sub> was tested in a real-life scenario (42% anatase and 38% rutile)<sup>72</sup> and coated on outdoor limestone surfaces, it was found that the photocatalytic ability was almost totally reduced after one year. Also, the surface color of the limestone was changed by the end of the term of exposure. The massive influence of environmental factors such as humidity, temperature, and concentration of pollutants in the microstructure of the coating could influence photocatalytic activity. While these factors will be more limited in an indoor scenario, they cannot be ignored.<sup>73–75</sup>

The low-cost and anticorrosive properties of TiO<sub>2</sub>, its photocatalytic efficacy, and its ability to deactivate viruses, bacteria, and fungi make it one of the most attractive materials for surface coatings which, in many cases, must be spread over vast surface areas. The increased interest in TiO<sub>2</sub> NPs as coatings is demonstrated by the increase in articles per year from just under 20,000 to almost 50,000 from 2010 to date (Fig. 4).

With this review, we intend to highlight the latest research on NPs with applications in indoor facilities like hospitals or food processing areas focusing on TiO<sub>2</sub>-containing paints or coatings and the strategies followed to make them more effective in visible-light conditions while maintaining their durability.

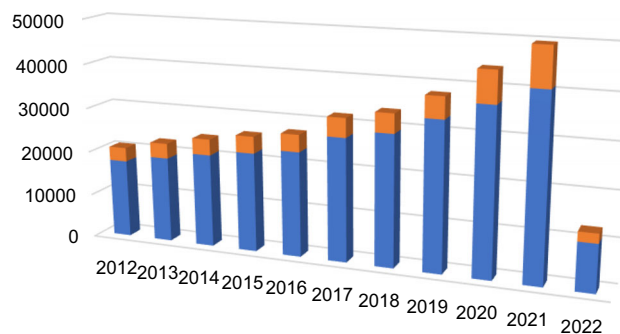


**Fig. 4:** Diagrams reporting the number of publications per year for the reported time ranges. (adapted from Web of Science, Clarivate Analytics; date of search: May 10, 2022)<sup>76</sup> using the following combinations of topic keywords: (a) TiO<sub>2</sub> or titanium dioxide and coatings or paints and antibacterial or antimicrobial or antifungal or antiviral or visible light; the number of publications corresponding to the orange portion of the bar have been obtained narrowing the search adding UV as a topic keyword

## Toward visible-light activity–doping

### *Metal dopants: reducing band gap energy*

It was mentioned before that the large bandgap of pristine TiO<sub>2</sub> NPs (3–3.2 eV) makes it impossible to employ its photocatalytic properties in visible-light conditions; this can only be achieved by the incorporation of dopants that affect the electronic band structure enough to promote visible-light absorption and a red light shift in the bandgap. The valence band of titania consists of hybridized states of oxygen 2p orbitals and titanium 3d orbitals, while the conduction band consists of titanium 3d orbitals. TiO<sub>2</sub> can be doped with either metals or non-metals or combinations of them.

The doping of TiO<sub>2</sub> with transition elements with partially filled d-orbitals alters the charge transfer properties in such a way that photogenerated carriers are successfully separated, producing a shift in absorption properties. This happens when Ti<sup>4+</sup> is replaced in the TiO<sub>2</sub> lattice by a transition metal, creating a new energy state in the band gap of TiO<sub>2</sub>. The localized d-electron state of the transition metals captures electrons from the titania valence band, suppressing the recombination of electrons and photogenerated holes. Transition metal ions like Mo<sup>6+</sup> have a very similar radius to Ti<sup>4+</sup>, affording easy substitution and a narrow bandgap.<sup>77</sup>

The incorporation of rare earth metals into the TiO<sub>2</sub> crystal lattice can also activate visible light since the large mismatch between the charge and ionic radii between the dopants and the titania affords lattice defects. Rare earth dopants with 4f, 5d, and 6s electrons introduce impurity energy levels by introducing orbitals between the conduction and valence bands which act as trapping centers for photogenerated species.<sup>78, 79</sup>

Yu and co-workers synthesized V-doped TiO<sub>2</sub> NPs by the sol-gel hydrolysis method using titanium butoxide (Ti(OBu)<sub>4</sub>) and vanadyl acetylacetonate (VO(acac)<sub>2</sub>) as the precursor and dopant, respectively. The bandgap energy of 0.45% V-doped TiO<sub>2</sub> NPs was reduced to 2.34 eV with a distinct redshift from 3.25 eV. The photocatalytic activity of these NPs exhibited two times higher enhanced visible-light-induced photocatalytic performance compared to the pristine TiO<sub>2</sub> NPs when used to reduce methylene blue.<sup>80</sup>

Some noble-metal NPs (Ag, Au, Cu, Pt and Pd) can absorb light from the visible to the near-infrared range due to localized surface plasmon resonance (LSPR). The term LSPR describes the oscillation of metal particle-free electrons. Free electrons are set into oscillatory vibrations when NPs are irradiated with a resonant frequency similar to the oscillating frequency.<sup>81</sup>

When dopants like Au and Ag NPs are used, LSPR generates hot electrons and holes in the TiO<sub>2</sub> conduc-

tion band under visible light. The holes can capture conduction electrons of TiO<sub>2</sub>, reducing the charge recombination processes.

### *Non-metal dopants: reducing band gap energy*

The incorporation of non-metals also resulted in the narrowing of the band gap energy and, accordingly, having a positive effect on the photocatalytic activity of the doped TiO<sub>2</sub> composite in visible light. The ionic radii of nitrogen and oxygen are comparable; thus, doping TiO<sub>2</sub> via the replacement of oxygen with nitrogen does not have a high formation energy barrier.

When nitrogen is incorporated into the crystal lattice of TiO<sub>2</sub>, its spectral response is extended to the visible region<sup>82, 83</sup> because of the position of the N 2p state above the valence band.<sup>84</sup> When TiO<sub>2</sub> fiber is doped with N during the synthesis, the band gap energy was reduced from 3.39 to 3.01 eV. This resulted in the improved photocatalytic degradation of methylene blue under visible light.<sup>85</sup> In a review, Du et al. emphasized that doping TiO<sub>2</sub> with N reduces the recombination efficiency of photoinduced charge carriers.<sup>86</sup> However, the photocatalytic reaction rates of these N-doped TiO<sub>2</sub> NPs are still low due to poor visible-light absorption (thus, ideal band-to-band absorption is not yet achieved).

Doping TiO<sub>2</sub> with sulfur has been reported to be either cationic or anionic. Thus, sulfur can replace either Ti ions (see Fig. 5 for comparing the pristine and substituted TiO<sub>2</sub> crystal cell unit) or lattice oxygen, respectively.<sup>87, 88</sup> Both cases resulted in improved photocatalytic activity. The visible-light activity of S-doped TiO<sub>2</sub> is caused by the band gap narrowing from

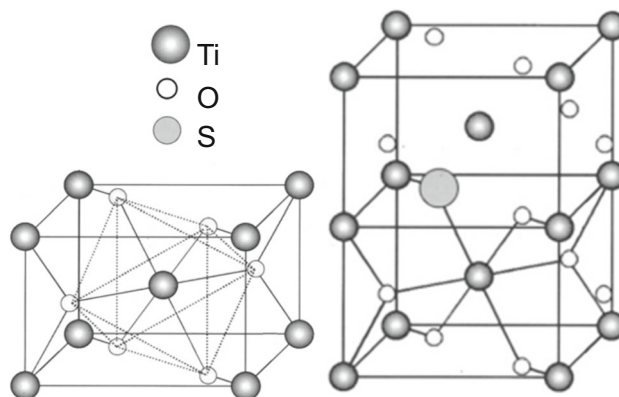


**Fig. 5:** The cell unit of (left) pristine rutile TiO<sub>2</sub> and (right) cell unit where one of the oxygen molecules was replaced with a sulfur molecule. Dark spheres: Ti; white spheres: O; gray spheres: S. Reprinted from Umebayashi, T. et al. Sulfur-doping of rutile-titanium dioxide by ion implantation: Photocurrent spectroscopy and first-principles band calculation studies. *J. Appl. Phys.* 2003, 93, 5156–5160.<sup>87</sup> Copyright (2003), with permission from the American Institute of Physics

mixing the S 3p and O 2p states. It has been shown that S-doped TiO<sub>2</sub> can be effectively used as visible-light photocatalysts to kill bacteria (*M. lylae*).<sup>89</sup>

The band gap energy can be drastically reduced when TiO<sub>2</sub> is doped with red phosphorus (P<sub>4</sub>) from 3.2 eV to 2.5 eV.<sup>90</sup> It is proposed that the redshift obtained for the band gap energy of black phosphorus-doped TiO<sub>2</sub> is due to the replacement of Ti<sup>4+</sup> with pentavalent P.<sup>91</sup> A review article is available on the band gap narrowing and photocatalytic activity of C-, N-, and S-doped TiO<sub>2</sub>.<sup>92</sup>

Doping of photocatalysts with carbon dots (CDs) has been reported to improve their ability to absorb long-wavelength photons in the visible-light region<sup>93</sup> by inhibiting the recombination of the photoelectron-hole pairs.

CDs were grown on TiO<sub>2</sub> sheets during a hydrothermal process using ammonium citrate (see Fig. 6 for an illustration of the preparation).<sup>94</sup> The CDs act as solid-state electron mediators, producing a highly effective visible-light photocatalyst to degrade aquatic pollutants.

When macro-mesoporous TiO<sub>2</sub> nanospheres were doped with carbon CDs (30% doping), they formed nanocomposites which were more successful in degrading methylene blue under visible light than the undoped TiO<sub>2</sub> sample.<sup>95</sup> In a different study, carbon quantum dots (CQDs) were randomly embedded in mesoporous TiO<sub>2</sub> using a solgel-based approach without destroying the mesopores.<sup>96</sup> This enhanced the visible-light photocatalytic activity of the TiO<sub>2</sub> composite, as shown by the 98% removal of methylene blue compared to the 5% removal using the pristine TiO<sub>2</sub> under the same conditions. The deposition of CQDs on TiO<sub>2</sub> also resulted in an effective photocatalyst for wastewater treatment.<sup>97</sup>

The preparation of a CQD-modified TiO<sub>2</sub> composite via a hydrothermal reaction resulted in a photocatalyst which could evolve hydrogen under visible light four times more efficiently than pure TiO<sub>2</sub>.<sup>98</sup> It was

proposed that the CQDs photosensitized the TiO<sub>2</sub> to be able to respond under visible light, resulting in a dyad structure which could evolve hydrogen. When this CQD-modified TiO<sub>2</sub> composite was exposed to UV-visible irradiation, the CQD took on a different role, acting as an electron reservoir. This results in the more efficient separation of photoelectron-hole pairs of TiO<sub>2</sub>.

Some researchers doped the CQDs with other non-metals, such as S, N and P, and then incorporated them on TiO<sub>2</sub>, resulting in even more superior photocatalysts.<sup>99, 100</sup>

### Photocatalytic activity

Nanomaterials exhibit exceptional photocatalytic activity making them a choice material for applications such as environmental remediation, decomposition/degradation of harmful substances (such as dyes, industrial effluent, bacteria, organic toxins, and metal ions), and renewable energy sources. Factors influencing the photocatalytic ability of nanoparticles like TiO<sub>2</sub> include surface area, crystallinity, crystal phase, crystal shape (facet and morphology), crystallite size, and dopants.<sup>101</sup>

The review of Padmanabhan et al. discussed how the different facets of TiO<sub>2</sub> NP surfaces could be engineered to obtain better photocatalysis.<sup>102</sup> To improve the visible-light photocatalytic activities of the TiO<sub>2</sub> (101) surface, Han et al. used DFT calculations to study TiO<sub>2</sub>(101) facets doped with 4d transition metal atoms by systematically investigating the geometric structures, doping methods, and the optical properties of the doped surfaces. They found that the visible-light absorption can be enormously increased by doping with Y, Zr, Nb, Mo, and Ag and only weakly increased by doping with other 4d transition metals. Y and Ag-doped NPS showed the most improvement of the TiO<sub>2</sub>(101) surfaces among all the elements studied.<sup>103</sup>



Fig. 6: An illustration of the procedure used to prepare carbon dots/TiO<sub>2</sub> sheets. Reprinted from: Shen, S. et al. Construction of carbon dots-deposited TiO<sub>2</sub> photocatalysts with visible-light-induced photocatalytic activity to eliminate pollutants. *Diam. Relat. Mater.* 2022, 124, 108,896,<sup>94</sup> (copyright 2022) with permission from Elsevier

By replacing the microstructural building units of hard biotemplated TiO<sub>2</sub> typically obtained from sol-gel methods, Jiang et al.<sup>104</sup> used solvothermal techniques to prepare both convex and concave nanotextured surfaces impregnated on biotemplates (tobacco stems) using tetrabutyltitaniumdioxide, glycerine or HF, respectively, with isopropanol as solvent. The convex material had the highest visible-light photoactivity for the reduction of tetracycline, more than 20 times faster than the new TiO<sub>2</sub> material. XPS measurements showed that the catalysts had advantageous carbon impurities obtained from the biomass during synthesis. Also, the bandgap values of this material were calculated as 2.89 eV, confirming the sensitization of biomass carbon dopants.

The photocatalytic performance of TiO<sub>2</sub> can be enhanced even further by incorporating a dopant. Ye et al. produced C–TiO<sub>2</sub> nanocomposites by a facile calcination approach and acid etching using starch as the carbon source and Fe<sub>2</sub>O<sub>3</sub> as a graphitization catalyst precursor. After calcination at 800°C, the iron species were removed by washing with hot HCl. The photocatalytic degradation rate of tetracycline was six times higher than pristine TiO<sub>2</sub> under visible light. Also, after seven cycles, the material showed no decrease in photocatalytic activity.<sup>105</sup>

Lee et al. synthesized a hybrid nanocomposite composed of one-dimensional N-doped TiO<sub>2</sub> nanotubes (N-TNTs) and two-dimensional graphitic carbon nitride nanosheets (g-CNNs) to obtain visible-light photocatalysis. They got 98% degradation of rhodamine B after 150 min of exposure to solar lighting. Moreover, the composites were still as effective after four cycles, indicating durability and stability.<sup>106</sup>

When designing a photocatalyst containing at least two entities, attention to optimization of the molar ratio and the effect of calcination temperature on the photocatalytic properties is an important aspect often under-investigated. N-doped TiO<sub>2</sub> NPs synthesized via the glycerol-assisted sol-gel technique and with variation nitrogen-to-titanium (N:Ti) molar ratio, calcination temperature, calcination duration and TiO<sub>2</sub> loading were investigated for the photodegradation of formaldehyde vapor under visible light. All the N-doped catalysts exhibited a narrow bandgap (2.64–2.50 eV) and small particle sizes ranging from 23.12 to 25.17 nm. The photodegradation results were the highest (70.59%) for an N:Ti molar ratio of 20:1. N-doped TiO<sub>2</sub> calcined at 300°C for 1 h provided the highest catalytic efficiency.

It is widely accepted that anatase TiO<sub>2</sub> has better photocatalytic properties, but rutile TiO<sub>2</sub> is cheaper and chemically more stable. By incorporating Mn and graphene (G) into TiO<sub>2</sub> nanowires (T(G–Mn) NW) in a two-step process (facile electrospinning followed by a hydrothermal process),<sup>107</sup> it is possible to manipulate the material's crystal structure by changing the annealing temperature (see Figs. 7a–7f for the SEM images). At 550°C, a mixture of rutile and anatase was

confirmed by powder diffraction methods. By elevating the temperature to 800°C, only pure rutile T(G–Mn) NW was obtained. Interestingly, this was also the photocatalyst with the superior photocatalytic performance under visible-light reduction of NO<sub>x</sub> (see Figs. 7g and 7h for the comparative graph of photocatalytic efficiency). The authors contributed this to the variations in oxygen vacancy concentrations and the Ti–O defects that arise because Mn and G are included in the crystal lattice.

Combining Cu<sub>2</sub>O, graphene, and TiO<sub>2</sub> also gives excellent photocatalytic properties and good stability. TiO<sub>2</sub>/G/Cu<sub>2</sub>O nanosheets were fabricated on carbon fiber in a three-step process and evaluated the degradation of rhodamine B (RhB) in visible-light conditions.<sup>108</sup> After 180 min, the RhB was degraded by 80%, compared to TiO<sub>2</sub>/Cu<sub>2</sub>O nanosheets which degraded RhB by 40%. The graphene acts as an electron sink and accepts photoelectrons, preventing the formation of photoelectron-hole pairs.

Fe/TiO<sub>2</sub> and Co/TiO<sub>2</sub> NPs were synthesized by sol-gel methods, and their photocatalytic activity under visible-light degradation of carbamazepine has been evaluated and compared to pristine TiO<sub>2</sub> NPs.<sup>109</sup> Under UV-A light, the 1 wt% Fe/TiO<sub>2</sub> NPs outperformed the other materials substantially, reaching 96.9% degradation after 240 min. However, when the same reactions were performed in visible-light conditions, all three catalysts performed poorly, with only 12.54% of carbamazepine degradation obtained after 240 min using the 1 wt% Fe/TiO<sub>2</sub> NPs (again, the best performer).

The physicochemical properties of noble-metal nanoparticles determine the photocatalytic activity of TiO<sub>2</sub>-modified NPs. TiO<sub>2</sub> modified with mono- and bimetallic nanoparticles of Pt, Cu, and Ag were prepared using chemical and thermal reduction methods. Their photocatalytic activity was examined for 2-propanol oxidation and hydrogen generation processes. The effect of size, metal type, and content of the different NPs on biocidal activity was also evaluated. The synthesis method significantly influenced the size of the nanoparticles but was also determined by the type of metal used. For example, the thermal reduction method produced smaller NPs than the chemical methods when Pt was used, but the opposite was found for Ag. Using light-emitting diodes, the biocidal test results indicated that Ag NPs obtained by chemical methods had the highest activity.

To develop less laborious processes to modify the surface of anatase TiO<sub>2</sub> with gold or silver, Salomatina et al. added the calculated amount of NP precursors to acetic acid solutions of chitosan and then dispersed TiO<sub>2</sub> particles in the solution, followed by enzymatic destruction of chitosan by chitosanase. As a result, Au and Ag NPs of small-size parameters were deposited on the TiO<sub>2</sub> surface. As expected, the photocatalytic activity of the prepared NPs was not as effective under visible light as with UV light. This was attributed to the fact that the excitation of electrons in the valence band

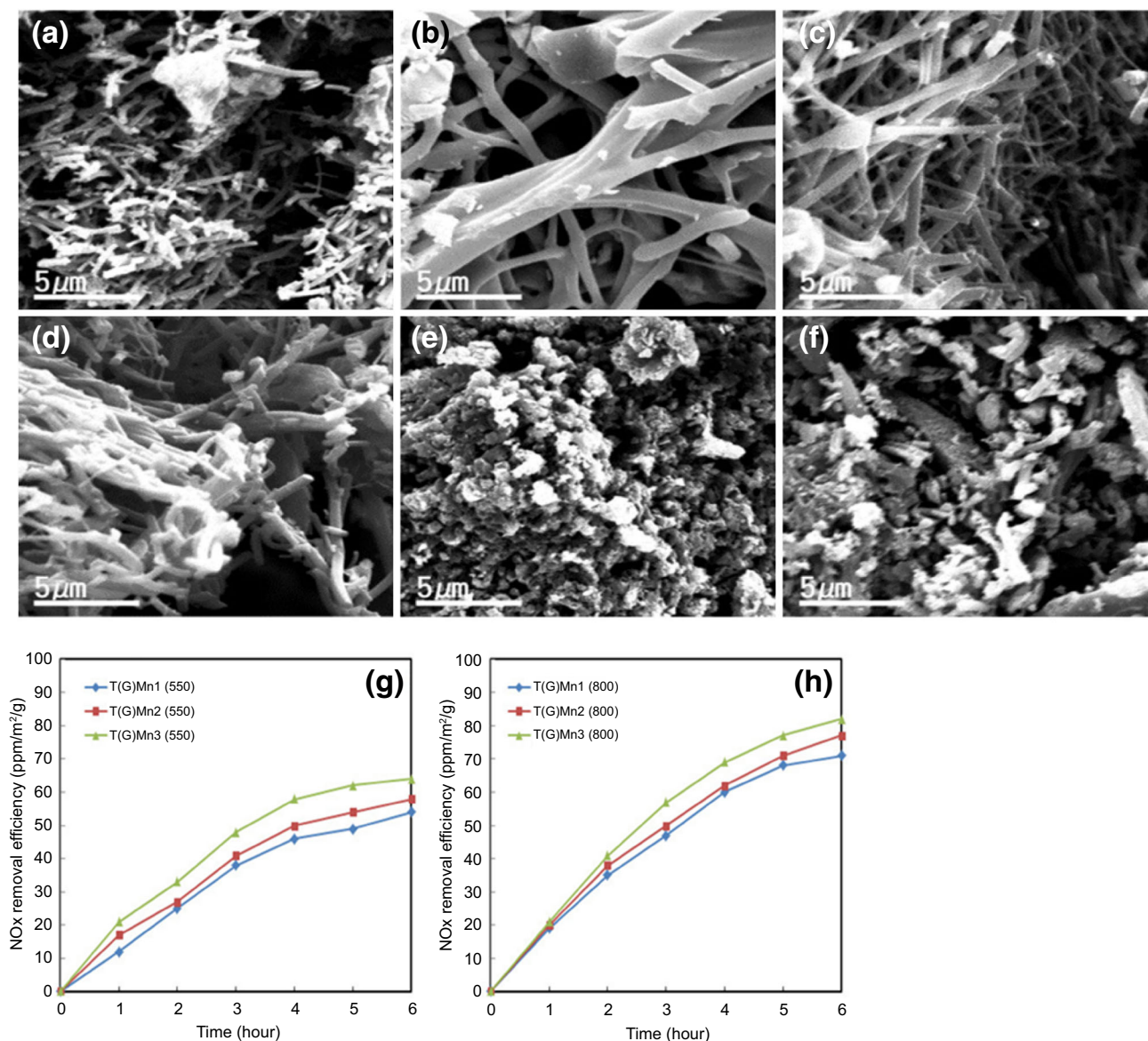


**Fig. 7:** SEM images of T(G-Mn)1 annealed at (a) 550°C and (d) 800°C, T(G-Mn)2 annealed at (b) 550°C and (e) 800°C, and T(G-Mn)3 annealed at (c) 550°C and (f) 800°C, showing the structure manipulation. The graphs indicate the photocatalytic efficiency for the removal of NO<sub>x</sub> by different T(G-Mn) annealed at (g) 550°C and (h) 800°C. Reprinted from: Lee, J.-C., et al. Manganese and graphene included titanium dioxide composite nanowires: fabrication, characterization and enhanced photocatalytic activities. *Nanomaterials* 2020, 10, 456,<sup>107</sup> (copyright 2020) with permission from MDPI

under UV light was imparted with excess energy, which increased their lifetimes at impurity-defect levels and in the conduction band.<sup>110</sup>

Zhang et al.<sup>111</sup> fabricated a composite photocatalyst composed of polyethylene terephthalate (PET) filaments loaded with Ag-N co-doped TiO<sub>2</sub> nanoparticles and sensitized with the water-insoluble disperse blue 183 dye for applications in water purification. For this review, the superior photocatalytic activity of the dye-sensitized Ag-N co-doped TiO<sub>2</sub>-coated PET filaments need mentioning as this technology can be transferred to indoor applications. The photodegradation results of methyl orange (MO) dye solution showed that the

positive holes, ·OH- and ·O<sub>2</sub><sup>-</sup> radicals, were the main reactive radical species under visible-light catalysis. Further, these filaments did not lose photocatalytic activity under repetitive experiments.

The microbial synthesis of nanoparticles is gaining increasing attention due to its more straightforward, greener, and economical approach. The synthesis of titanium dioxide embedded silver oxide nanocomposite structures (AgO/Ag<sub>2</sub>O@TiO<sub>2</sub>) using a cell-free growth culture supernatant of the bacteria *Alcaligenes aquatilis* was recently reported.<sup>112</sup> Briefly, the cell-free supernatant was obtained by centrifugation after growing the culture in a nutrient broth at room

temperature. After this,  $\text{AgNO}_3$  was added and stirred to reduce the silver. The formed nanoparticles were washed and added to more of the supernatant and hexafluorotitanate ( $\text{K}_2\text{TiF}_6$ ) and kept at room temperature for 4 h while stirring. The fabricated photocatalyst had a band gap of 1.75 eV and was able to degrade the Reactive Blue-220 dye almost completely under visible light in 90 min.

### **Antibacterial activity: crystal properties and dopants for visible-light photocatalytic disinfection**

Titanium dioxide nanoparticles are considered attractive antibacterial materials since they are chemically stable, not toxic, economical to produce, and, most importantly, they are photocatalytically active, thus producing ROS. Damp environments are excellent sources for microbe growth, assisting the need for water during ROS production.

The efficiency of  $\text{H}_2\text{O}$  adsorption on  $\text{TiO}_2$  surfaces determines the generation of ROS and, in turn, antimicrobial effects. Theoretical and experimental studies showed that the molecular adsorption of  $\text{H}_2\text{O}$  prefers to take place on anatase (101) surfaces, but the chemical reactivity for water decomposition occurs in the order  $(001) > (100) > (110) > (103) > (101)$ .<sup>113</sup> The surface potentials of the facets determine whether a facet will become an oxidation site or a reduction site during photocatalysis. For example, (110) is the reduction and (001)/(111) are the oxidation sites in faceted rutile crystals, respectively. Furthermore, the charge separation of photogenerated species is strongly facet dependent. In other words, the morphology of  $\text{TiO}_2$  NPs determines their photocatalytic behavior. Phadmanabahn et al.<sup>102</sup> discussed how this morphology can be controlled by introducing high-energy facet stabilizing agents like amino or carbonyl groups, promoting the growth of certain facets above others.<sup>102</sup> Recently, Chen et al. showed how vital the facet-dependent contact of  $\text{TiO}_2$  with graphene is for the photolytic behavior (see Fig. 8 for the proposed mechanism).<sup>114</sup> The morphology of  $\text{TiO}_2$ /graphene hybrids synthesized via a hydrothermally modified solgel method can be varied between nanoellipsoids with high-energy facets and nanoellipsoids exposing low-energy facets by just changing the quantity of water that determines the hydrolytic steps during crystal growth, as was shown by Phadmanabahn et al. recently.<sup>115</sup>

The effective generation of ROS can also be obtained by combining the charge separation properties of graphene with the surface plasmon resonance effects facilitated by Ag NPs. In this regard, an Ag/ $\text{TiO}_2$ /rGO nanohybrid (rGO = reduced graphite oxide) was recently reported for its excellent antibacterial properties and activity toward *E. coli* and *S. aureus* and its self-cleaning ability. A 100% disinfection

of the bacterial environments was obtained within 180 min of visible-light irradiation.<sup>116</sup>

Coating photocatalytic  $\text{TiO}_2$  NPs via an aerosol method to glass resulted in 99% efficiency antibacterial and antibiofilm activities against *S. aureus*.<sup>117</sup>

The antimicrobial efficacy of copper (Cu)-doped  $\text{TiO}_2$  ( $\text{Cu-TiO}_2$ ) was evaluated against *E. coli* and *Staph. aureus* under visible-light irradiation. The doping of  $\text{TiO}_2$  was obtained with a solgel method, using 0.5 mol% Cu. UV-Vis results indicated that the band gap was reduced to 2.8 eV. Through density functional theory (DFT) studies, the existence of oxygen vacancies created by the substitution of  $\text{Ti}^{4+}$  by  $\text{Cu}^+$  and  $\text{Cu}^{2+}$  ions was confirmed. A significantly high bacterial inactivation (99.9999%) was attained in 30 min of visible-light irradiation by  $\text{Cu-TiO}_2$ .<sup>118</sup>

In another study, silver and gold were used to modify commercial titania. They were tested for their antibacterial (*Escherichia coli* (*E. coli*)) and antifungal (*Aspergillus niger* (*A. niger*), *Aspergillus melleus* (*A. melleus*), *Penicillium chrysogenum* (*P. chrysogenum*), *Candida albicans* (*C. albicans*)) activity under visible-light irradiation and in the dark. The Ag-modified NPs showed remarkably high antibacterial activity and decomposed bacterial cells under visible-light irradiation. The gold-modified samples were almost inactive against bacteria in the dark but showed a significant bactericidal effect under visible-light irradiation. This was attributed to the plasmonic excitation of titania by the localized surface plasmon resonance of gold. The antifungal activity tests showed efficient suppression of mycelium growth by bare titania and suppression of mycotoxin generation and sporulation by gold-modified titania.<sup>119</sup>

On their own, CQDs have been reported to show bacteriostatic and bactericidal properties under photo-dynamic conditions.<sup>120</sup> The combination of CQDs and  $\text{TiO}_2$  has resulted in better photocatalytic antibacterial activity than pristine  $\text{TiO}_2$ .<sup>97</sup> The antibacterial properties of CQDs- $\text{TiO}_2$  reached 90.9% and 92.8% efficiency against the Gram-negative, Gram-positive *E. coli* and *S. aureus* strains under visible-light irradiation (see Fig. 9 for the TEM images of the cells).<sup>121</sup> The CQDs- $\text{TiO}_2$  nanocomposite could be recycled seven times.

### **Dopants in coatings and paints**

Several paints on the market worldwide are already enriched with  $\text{TiO}_2$  or doped  $\text{TiO}_2$  to degrade priority pollutants like NO. Unfortunately, while many of these paints can degrade NO by more than 80%, the formation of  $\text{NO}_2$  as a by-product is either ignored or neglected. To demonstrate this, Kotzias et al. used  $\text{TiO}_2$  doped with manganese (0.1 wt%) and were able to degrade NO up to 95% in indoor conditions using only visible light with a conversion efficiency of NO to  $\text{NO}_2$  of 2%. This was compared to commercial products, some of which showed up to 8% conversion (see

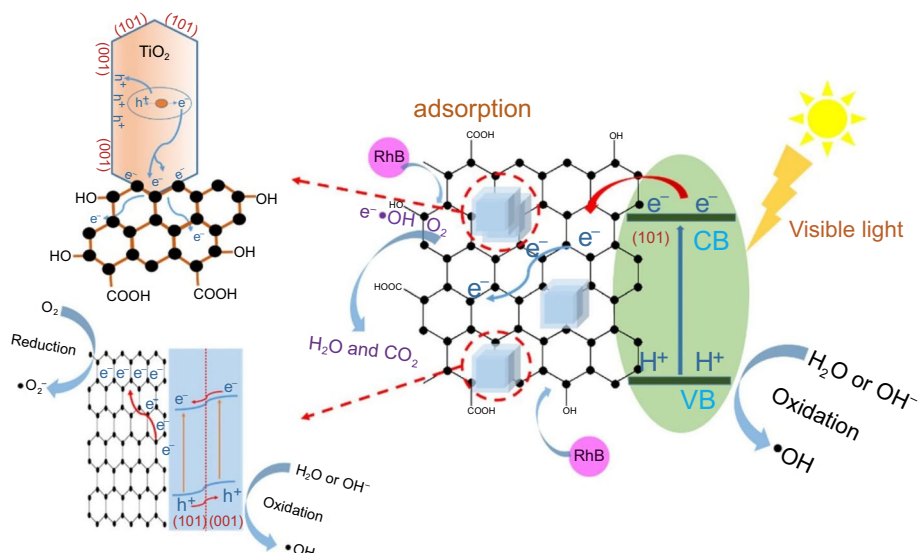


Fig. 8: The proposed mechanism of facet-dependent contact 3D/2D heterojunctions for photocatalytic reactions. Reprinted from: Chen, L. et al. One-step solid-state synthesis of facet-dependent contact  $\text{TiO}_2$  hollow nano cubes and reduced graphene oxide hybrids with 3D/2D heterojunctions for enhanced visible photocatalytic activity. *Appl. Surf. Sci.* 2020, 504, 144,353,<sup>114</sup> (copyright 2020) with permission from Elsevier

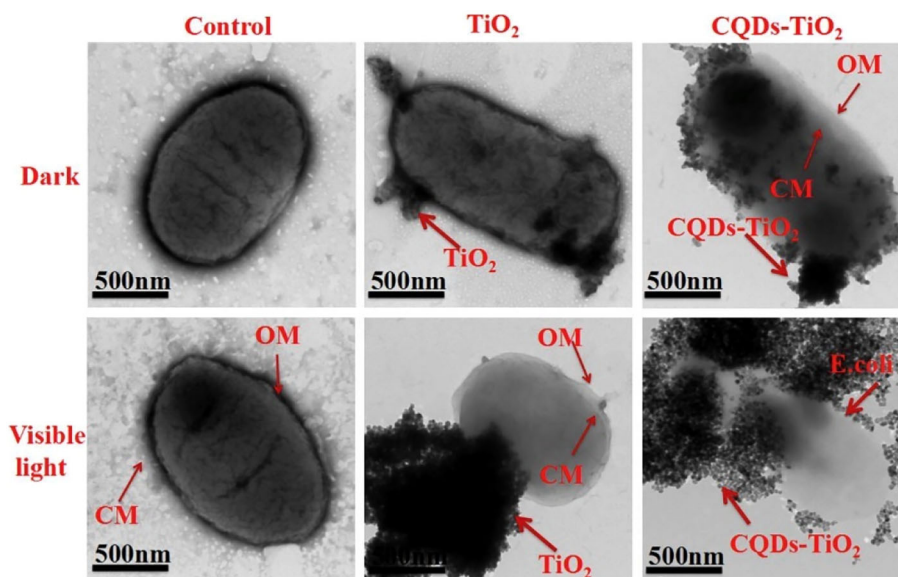


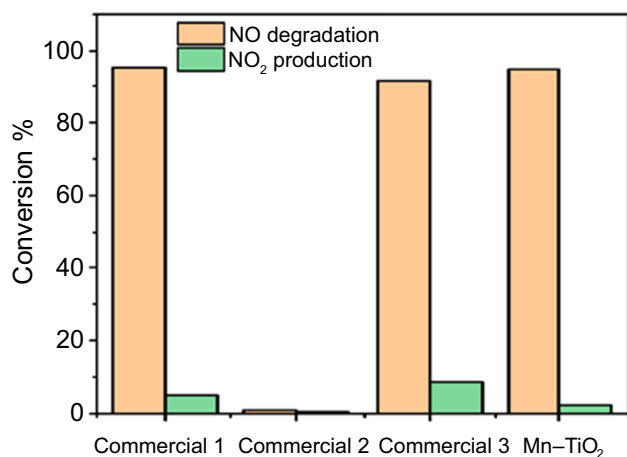
Fig. 9: The TEM images of *E. Coli* cells after introducing  $\text{TiO}_2$  and CQDs- $\text{TiO}_2$  and irradiation with visible light. Reprinted from: Yan, Y. et al. Carbon quantum dot-decorated  $\text{TiO}_2$  for fast and sustainable antibacterial properties under visible light. *J. Alloys Compd.* 2019, 777, 234–243,<sup>121</sup> (copyright 2019) with permission from Elsevier

Fig. 10 for the comparative graph).<sup>122</sup> This shows the importance of focusing on photocatalytic efficiency and minimizing the emission of harmful substances.

The synthesis of a superhydrophobic  $\text{WO}_3$ - $\text{TiO}_2$  nanorod (MWT) dispersed in polydimethylsiloxane (PDMS) for use as a building coating by spraying methods produced superior durability and antifouling properties even after 450 days of practical application on an outdoor surface. The excellent self-cleaning property of the coating was confirmed by the removal

and resistance to the adhesion of powder particles. The degradation efficiency under visible light decreased by 4.74% after the first five cycles due to the adhesion of oxidation products. This was restored after flushing with water.<sup>123</sup>

Salvadores et al. formulated photocatalytic paints using pristine anatase or carbon-doped anatase. The paints were tested in indoor and outdoor environments against acetaldehyde and NO, respectively. A photoreactor was irradiated with fluorescent lamps with



**Fig. 10: Graphs showing the percentage conversion from NO to NO<sub>2</sub> of several commercial products under visible-light illumination. Adapted from: Kotzias, D. et al. Smart surfaces: photocatalytic degradation of priority pollutants on TiO<sub>2</sub>-based coatings in indoor and outdoor environments-principles and mechanisms. *Materials (Basel)*. 2022, 15, 402,<sup>122</sup> (copyright 2022) MDPI**

wavelengths varying from 310 to 710 nm for the indoor experiment. The formulation of a carbon-doped sample showed the highest acetaldehyde conversion, reaching almost 60% in 60 min. The outdoor experiments under UV light showed that the conversion ability of the different paints all decreased substantially with time, possibly due to oxidation products forming on the surfaces.<sup>124, 125</sup>

Currently, most commercial self-cleaning window surface coatings can only be activated by UV light. Recently, Peeters et al. manufactured a transparent photocatalytic self-cleaning Au/TiO<sub>2</sub> coating that is activated in normal light conditions.<sup>126</sup> Pre-fabricated gold nanoparticles were made compatible with the organic medium of a TiO<sub>2</sub> solgel coating suspension, resulting in a one-pot coating suspension. Homogeneous, smooth, highly transparent, and photoactive gold-embedded anatase thin films were obtained through spin coating methods. A clear redshift (see Fig. 11 for the UV-Vis spectra) of the surface plasma resonance band was observed for embedded Au nanoparticles (626 nm) compared to the colloidal suspension of PVP-stabilized Au nanoparticles (521.5 nm). The fact that the Au NPs were partially or fully embedded in the TiO<sub>2</sub> matrix enhanced its photocatalytic performance. It should protect it against the detachment often observed when NPs are not embedded in the matrix.

Moongraksathum et al. demonstrated the antiviral capability of a silver-doped TiO<sub>2</sub> coating prepared using a solgel method and achieved photocatalytic activity under UVA and visible-light irradiation. A 1% wt concentration of Ag in the TiO<sub>2</sub> solgel formed the most photoactive coatings. They tested the antiviral capability of their coating (on a glass substrate) against

influenza A and enterovirus. They achieved a > 99.99% (> 4.17-log) reduction in viral activity after irradiation with a 15 W UVA lamp for 20 min.<sup>127</sup>

Salvadores et al.<sup>124</sup> used undoped and carbon-doped TiO<sub>2</sub> in different amounts in the formulation of water-based and pseudo-paints and tested them for degradation of acetaldehyde under indoor conditions using visible light. They also evaluated the degradation of NO<sub>x</sub> under outdoor conditions using UV light. All the carbon-doped samples could degrade the two contaminants in different light conditions. The paint with the maximum amount of carbon-doped TiO<sub>2</sub> produced the best conversion efficiency but not the highest quantum efficiency. This was obtained in paint with less doped carbon, making it the optimal formulation for energy use.

In another study, nanosized Cu<sub>x</sub>O clusters were grafted onto TiO<sub>2</sub> to provide antibacterial properties under dark conditions through the Cu(I) species in the clusters. Visible-light photocatalysis was afforded by the Cu(II) species, but the particles' color turned brown as the copper concentration increased. This is one of the challenges of doped NPs for paint applications.<sup>52</sup> However, Bucuresteanu et al. seem to have overcome this and produced a washable paint containing 2% Cu-doped TiO<sub>2</sub> manufactured by a solgel process in a paint factory. The paint was tested and compared to standard painted areas in a community hospital over one year and showed a complete decrease to having zero microorganisms in the catalytically painted ward. In contrast, the contamination in the regular wards remained the same.<sup>128</sup>

Co-doping TiO<sub>2</sub> with Cu and N via a solgel process for photocatalytic coatings on glass surfaces revealed that the doping narrowed the band gap energy and the antibacterial properties of TiO<sub>2</sub> against *E. coli* and *S. aureus* increased with increased dopant concentration (see Fig. 12 for cell culture images).<sup>129</sup>

A thin coating of TiO<sub>2</sub> NP was prepared by aerosol flame synthesis and direct thermophoretic deposition, which resulted in the formation of a superhydrophilic coating.<sup>130</sup> This coating could be activated by standard room illumination to inhibit *Staphylococcus aureus*.

When surfaces such as medical grade stainless steel 316L were coated with TiO<sub>2</sub> or SiO<sub>2</sub>-TiO<sub>2</sub> using soft lithographic and Dip-Pen Nanolithographic methods, a reduction of 60% bacterial (*Streptococcus mutans*) adhesion to the surface was observed.<sup>131</sup> Additionally, bacterial adhesion was reduced even further when exposed to UV light.

### **Dopants and incorporation into textiles**

Incorporating nanomaterials into textile surfaces has initiated the development of new advanced nanocomposite textile products. Preparing TiO<sub>2</sub> NPs containing textiles is relatively uncomplicated; however, insufficient anchoring of the TiO<sub>2</sub> NPs to certain fibers imposes complications regarding the leaching of the

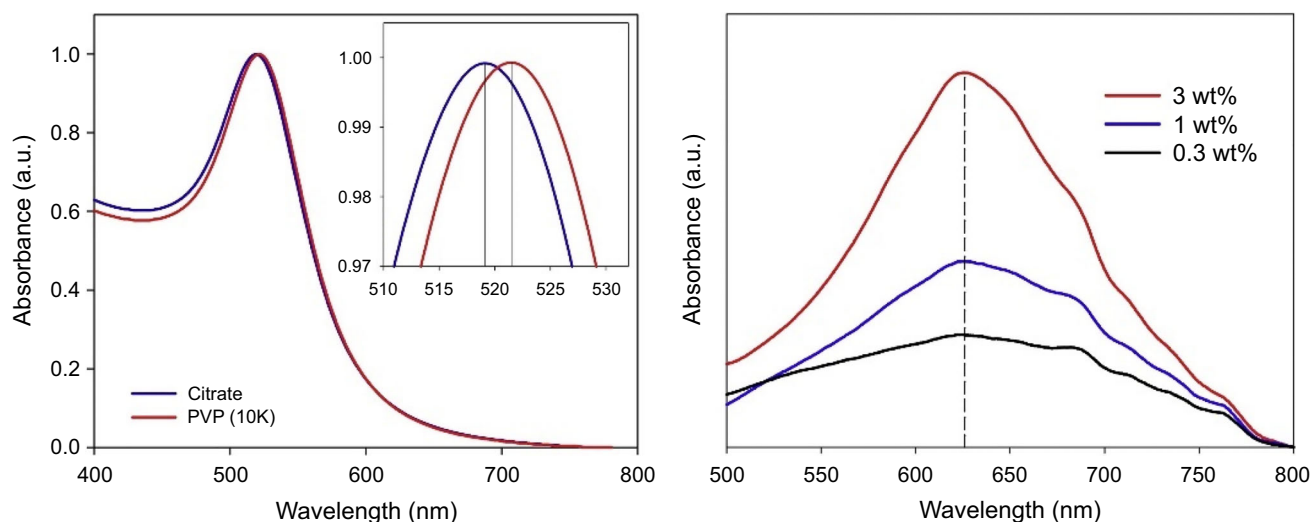


**Fig. 11:** Graphs showing the normalized UV-vis absorption spectra of (a) the colloidal Au NPs suspensions before (blue curve) and after (red curve) ligand exchange and (b) of the Au NPs modified films on glass with different loadings. A comparison of the two graphs clearly shows the redshift. Reprinted from: Peeters, H. et al. Plasmonic gold-embedded TiO<sub>2</sub> thin films as photocatalytic self-cleaning coatings. *Appl. Catal. B Environ.* 2020, 267, 118,654,<sup>126</sup> (copyright 2020) with permission from Elsevier (Color figure online)

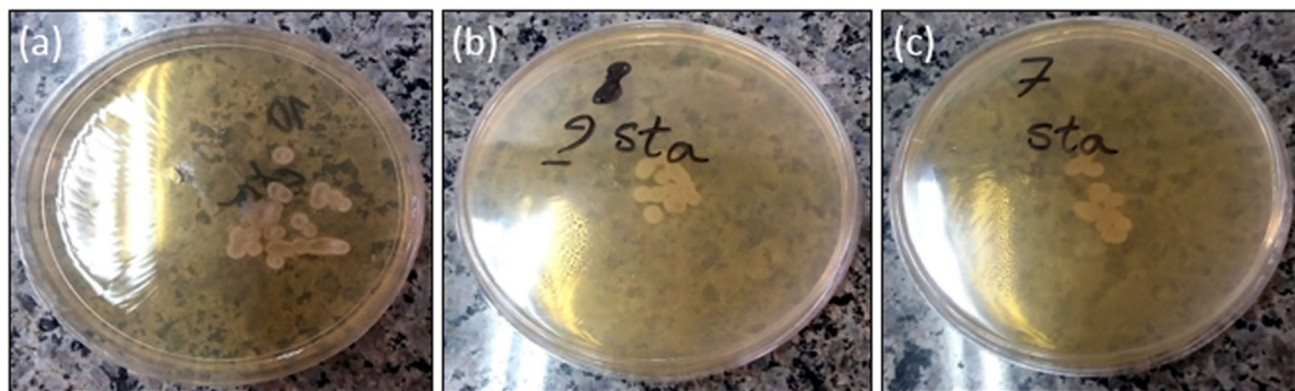


**Fig. 12:** Images of the *S. aureus* cells after irradiation with light from a methylene halide lamp radiation (a) the uncoated sample, (b) the undoped coating, and (c) the 0.75% Cu-N-doped coated sample. Reprinted from: Tahmasebizad, N. et al. Photocatalytic activity and antibacterial behavior of TiO<sub>2</sub> coatings co-doped with copper and nitrogen via sol-gel method. *J. Sol-Gel Sci. Technol.* 2020, 93, 570–578,<sup>129</sup> (copyright 2020) with permission from Springer Link

TiO<sub>2</sub> NPs and the stability and durability of these TiO<sub>2</sub> nanocomposite textiles.

To improve the bonding of a nanomaterial coating containing TiO<sub>2</sub> and SiO<sub>2</sub> onto polyester cotton and its visible-light activation, Gao et al.<sup>132</sup> synthesized TiO<sub>2</sub>/SiO<sub>2</sub>/graphene oxide nanocomposites and attached them onto the fabric using sonification (see Fig. 13 for the SEM images). The staining tests were performed using gentian violet and tested in sunlight. While samples containing TiO<sub>2</sub> or TiO<sub>2</sub>/SiO<sub>2</sub> and TiO<sub>2</sub>/GO could utilize the UV portion available in sunlight to decompose the stains somewhat, only TiO<sub>2</sub>/SiO<sub>2</sub>/GO was able to remove the stains within 8 h altogether. The photocatalytic activity against methylene blue was also investigated under visible-light conditions. Once again, the TiO<sub>2</sub>/SiO<sub>2</sub>/GO sample could

only decompose the dye within 24 h under visible light. To test the stability of the coating, the samples were washed with water, detergent, and petroleum ether for 45 min at room temperature under a constant stirring speed of 200 rpm, followed by drying in an oven at 60°C. This is equal to five home launderings at around 37°C. The TiO<sub>2</sub>/SiO<sub>2</sub>/GO sample maintained its photocatalytic activity, even after 5 and 10 washes. The authors also prepared similar materials using dip-pad methods instead of the ultrasonic bath. After each washing process, the dip-pad samples considerably lost their stain decomposition power, whereas the washing impact on the ultrasound samples was minor and negligible. These results could lay the foundation for future fabrications involving cotton-type fabrics.

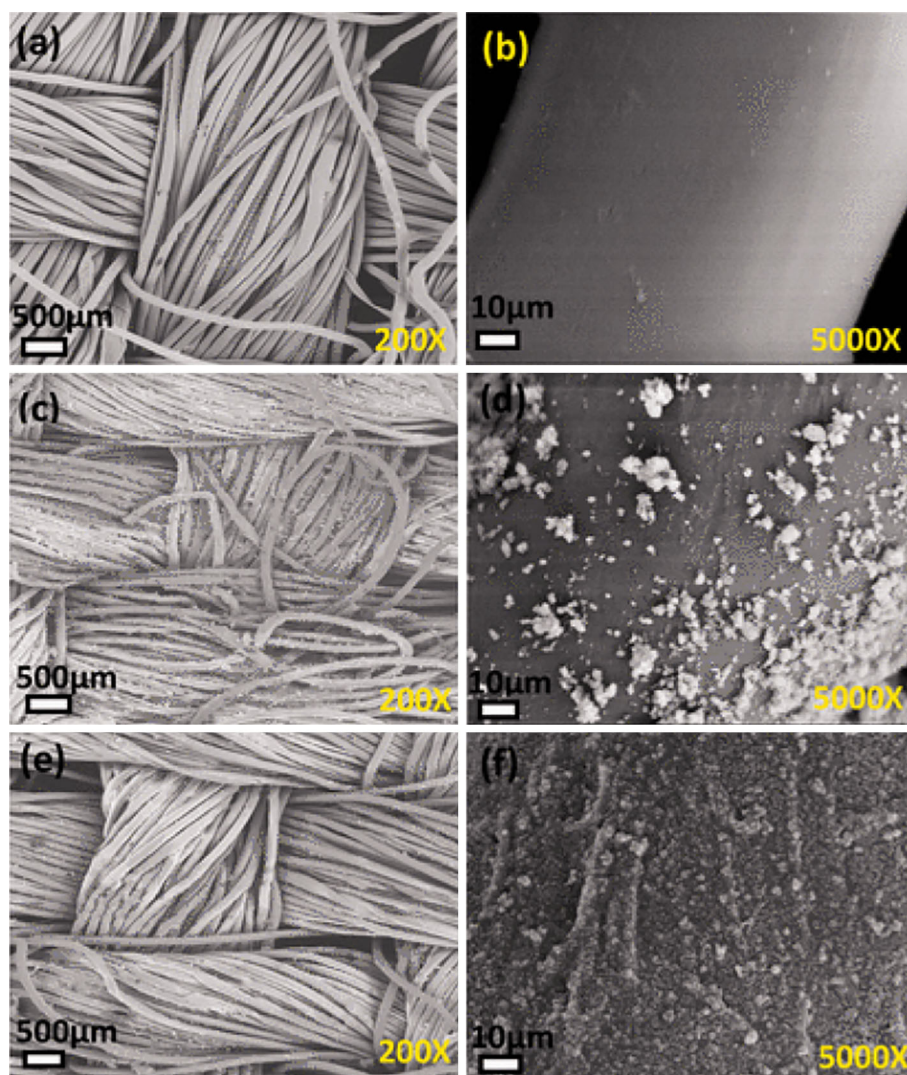


**Fig. 13:** The SEM images of polyester–cotton samples, (a and b) untreated, (c and d) treated with  $\text{TiO}_2$ , and (e and f) treated with  $\text{TiO}_2/\text{SiO}_2/\text{graphene oxide}$ . Reprinted from: Gao, J. et al. Durable visible-light self-cleaning surfaces imparted by  $\text{TiO}_2/\text{SiO}_2/\text{GO}$  photocatalyst. *Text. Res. J.* 2019, 89, 517–527,<sup>132</sup> (copyright 2019) with permission from SAGE Journals

The effects of ultrasound action on the polycondensation of  $\text{Ti-OH}$  were promoted through the generation of local hot spots during the implosion of bubbles, which in turn accelerates the crystallization process of  $\text{TiO}_2$ . Sonication also affords a more homogeneous number of nuclei with smaller particle sizes process (see Fig. 14 for the proposed mechanism).<sup>133, 134</sup>

Stan et al.<sup>135</sup> designed nanocomposites containing Fe, N-doped  $\text{TiO}_2$  NPs decorated on graphene oxide and treated cotton fibers with it for applications as self-cleaning, antimicrobial, and biocompatible textiles. Two different textiles, a knitted and woven cotton fabric, were used to evaluate the photocatalytic effect after different treatment parameters. For the first sample (KS1), the NPs were dispersed in sodium dodecyl sulfate (SDS) for 3 h in a sonic bath, after which the cotton knit was successively immersed at  $40^\circ\text{C}$  for 30 min. For KS2, SDS was not used to

disperse the NPs; for KS3, the cotton knit was pre-treated with polyvinylpyrrolidone in a sonic bath and, at  $60^\circ\text{C}$  then immersed in the same SDS solution used for KS1. The fourth sample, the woven fabric, was treated the same way as KS1.

As shown before, GO played a massive role in the increased interaction of the NPs with cellulose. Also, cell viability testing showed all the fabrics to be biocompatible. Regarding antimicrobial testing, KS1 exhibited the most potent antimicrobial activity against the gram-positive *E. faecalis* (77%), but *E. coli* could not be inhibited significantly after 24 h of contact.<sup>135</sup>

Naturally, frequent-touch surfaces in hospital environments are not only reduced to hard contact surfaces. Protective clothing and bedding also provide opportunities for developing new materials with visible-light photocatalytic activity. As an example, the preparation of  $\text{TiO}_2/\text{polyaniline}$ -coated kapok fiber

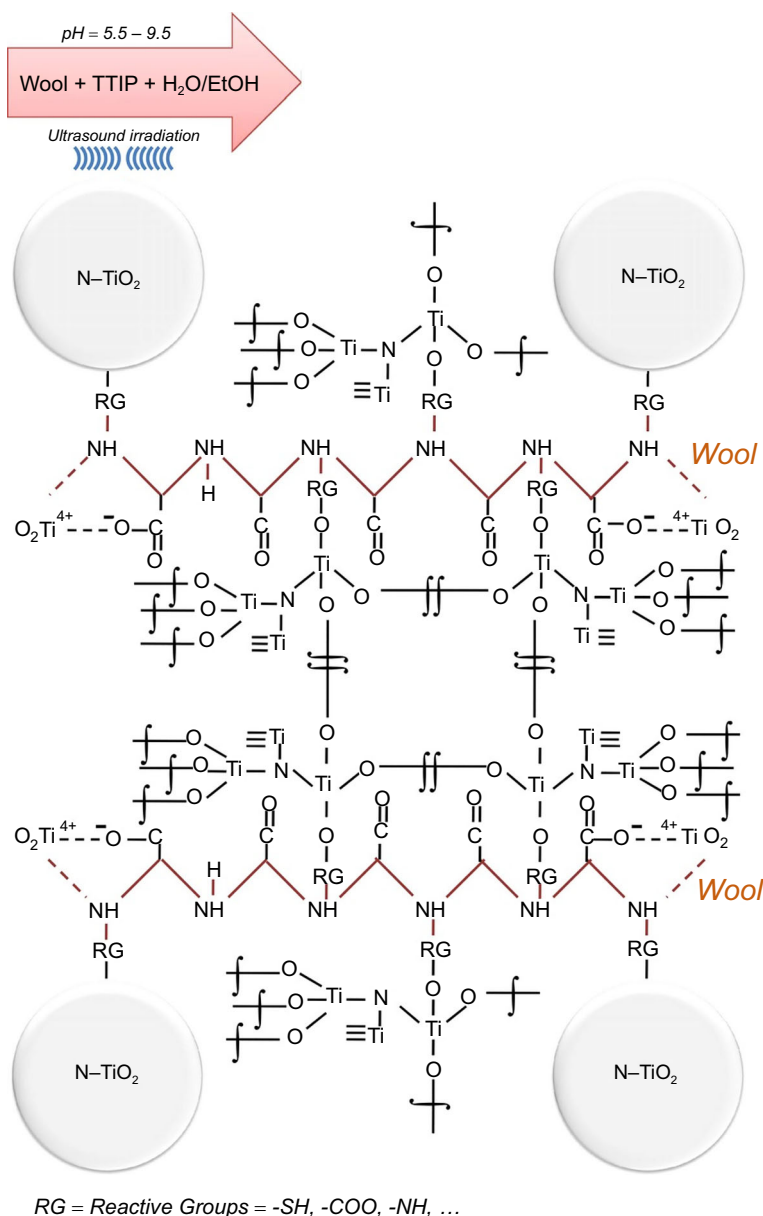


**Fig. 14:** The mechanism proposed for anchoring N-doped TiO<sub>2</sub> nanoparticle fiber was prepared by sonication. Reprinted from Behzadnia, A. et al. Rapid synthesis of N-doped nano TiO<sub>2</sub> on wool fabric at low temperature: introducing self-cleaning, hydrophilicity, antibacterial/antifungal properties with low alkali solubility, yellowness, and cytotoxicity. *Photochem. Photobiol.* 2014, 90, 1224–1233,<sup>134</sup> (copyright 2014) with permission from Wiley

(TiO<sub>2</sub>/PANI-KpF) nanocomposite for the visible-light-activated photodegradation of methyl orange (MO) and photoreduction of chromium (VI) [Cr(VI)] in an aqueous solution was published recently.<sup>136</sup> First, PANI-KpF was synthesized using the in situ polymerization of aniline monomer on the surface of kapok fibers in an acidic solution containing ammonium persulfate (APS) as the oxidizing agent. Hydrothermal methods were employed to immobilize the TiO<sub>2</sub> nanoparticles on the surface of PANI-KpF using titanium isopropoxide as the Ti source.

The new material reduced Cr(VI) entirely within 6 h and achieved 74.2% degradation of MO under normal light conditions. The antibacterial effects were investigated against *E. coli*, showing a 30% colony-forming-unit (cfu) reduction under visible-light conditions.<sup>136</sup>

Souza and co-workers' research<sup>137</sup> compared antiviral hydrophobic cellulose-based cotton to non-woven fabrics containing mesoporous TiO<sub>2</sub> hydrosols for potential use in healthcare and other frequent-touch environments. The virucidal effect of the different fabrics against Murine Coronavirus (MHV-3) and Human Adenovirus (HAdV-5) was evaluated under

indoor light irradiation. The visible-light photocatalytic activity was ascribed to doped carbon obtained from the acetic acid used in the solgel synthesis of the hydrosols. The results showed a 90% reduction of HAdV-5 and close to 99% of MHV-3 in non-woven fabric, and a 90% reduction of MHV-3 and no reduction of HAdV-5 in cotton fabric. The antiviral activity was attributed to the hydrophobic nature of the treated fabrics and the high surface area of the TiO<sub>2</sub> particles, which favor interaction with the viruses. While non-woven fabrics are usually only used once in a hospital environment; cotton fabrics are used more than once. The cotton fabrics in this study were washed once, and the virucidal effects were like the first test. However, it is accepted that the way the cotton material was tested (submerged in water and stirred under magnetizations not compared to normal washing conditions).<sup>137</sup>

In another study employing graphene oxide, cotton fibers were treated with graphene oxide and decorated with Fe-, N-doped TiO<sub>2</sub> nanoparticles. The results showed that the photocatalytic effect was dependent on the chemicals used to disperse the nanoparticles, the parameters of the treatment, and the fiber structure and composition of the material. By using double and triple treatments of the textiles, more uniform coverage with a more significant concentration of NPs could be obtained, resulting in a better photocatalytic effect under visible light. The materials' hydrophobicity also improved with the number of treatments due to the deposition of successive graphene layers, thereby warranting self-cleaning properties. To ensure a more robust material, some samples were covered with polyvinylpyrrolidone (PVP). The photocatalyst-treated cotton fabrics exhibited increased resistance to *Enterococcus faecalis* but not *Escherichia coli* colonization. This is probably due to *E. coli*'s thicker cell walls. Unfortunately, the authors did not mention exactly what the light conditions of this experiment were.<sup>135</sup>

Zhao et al. based their design of a visible-light photocatalyst on the synergy between Ag<sub>2</sub>O and TiO<sub>2</sub> by immobilizing Ag<sub>2</sub>O/TiO<sub>2</sub> nanocluster on a chitosan-modified polypropylene fiber which was able to kill 99.8% of *E. coli* upon irradiation with visible light within 60 min.<sup>138</sup> They also established that the bactericidal effects are mainly due to the photocatalytic process by comparing their results to a sample that was not irradiated.

Naturally, there is an urgent need for self-cleaning flexible materials in hospital environments. To attempt this, TiO<sub>2</sub>/SiO<sub>2</sub>/graphene oxide nanocomposites were sono-synthesized and sono-fabricated onto a cotton-polyester fabric through a facile one-step method. This fabrication method produced uniform, smooth coatings with few agglomerations. The functionalized samples' photocatalytic activity was tested through a gentian violet stain removal test and then photodecomposition of methylene blue under visible light and tested again after 10 washes to check on its durability. Furthermore, even after 10 washes, the samples virtually maintain this functionality. The fabrics were also compared with

similar materials produced by the usual dip-coat method and showed much better washability. This indicates that stronger bonding between the fabrics and the nanocomposites was established during sonification, probably due to the generation of transient localized hot zones formed by the microturbulence and shock waves.<sup>132</sup>

Pakdel et al.<sup>139</sup> formulated coatings composed of flowerlike particles of either TiO<sub>2</sub> or N-doped TiO<sub>2</sub> (see Fig. 15a for the SEM image) and combined it with polydimethyl siloxane (PDMS) polymer using a facile dip-coating method. The self-cleaning performance of the fabrics was assessed based on their superhydrophobicity and effective removal of oil-based stains under simulated sunlight. The water contact area (WCA) of the TiO<sub>2</sub>/N/PDMS coating was calculated as 157°, indicative of its hydrophobic properties (see Figs. 15b–15d for the WCA image). Furthermore, the coated fabric decomposed and absorbed oil-based stains after 30 min of irradiation, revealing its photocatalytic activity. The results that stand out are that the developed fabrics showed high robustness against chemical and physical durability tests repeated 50 times. Washability was not tested, though, and will be necessary for future applications.

### **Antimicrobial activity of TiO<sub>2</sub> in coatings and paint**

Another attractive strategy for improved antimicrobial activity is by controlling the structure composition of metal nanomaterials. Bimetallic alloys or core-shell nanoparticles generally are superior in antibacterial activity to nanoparticles comprised of individual metals because the introduction of surface strain and electronic coupling between the constituent atoms in bimetallic nanoparticles can significantly improve specific properties (see Fig. 16 for the SEM images of the treated bacterial cells).<sup>140</sup> This will be illustrated with the recent advances in the field discussed in the following paragraphs.

One such example is nanoclusters of Cu(I)/Cu(II) grafted onto TiO<sub>2</sub>, which were effective on both the antibacterial and antiviral properties, even under dark conditions. The optimum content of Cu<sup>I</sup> in the Cu<sub>x</sub>O nanoclusters was 56% (Cu<sup>I</sup>/Cu<sup>II</sup> = 1.3). Another example is the synthesis of a core-shell structure containing Fe/TiO<sub>2</sub> which was synthesized by solgel methods. The photocatalytic degradation of methylene blue reached 98% under UV light irradiation within 5 h, compared to 85% under visible light during the same period.<sup>141</sup>

Ferreira et al. investigated the effect of Co and N-doped TiO<sub>2</sub> NPs through an improved hydrothermal method. The photocatalysts were evaluated for their photocatalytic activity in UV, visible, and ambient light conditions. Their antimicrobial activities were considered against three different types of bacteria, *S. aureus*, *E. coli* and *L. pneumophila*, Gram-positive, Gram-negative, and a major waterborne pathogen.<sup>142</sup> Inter-

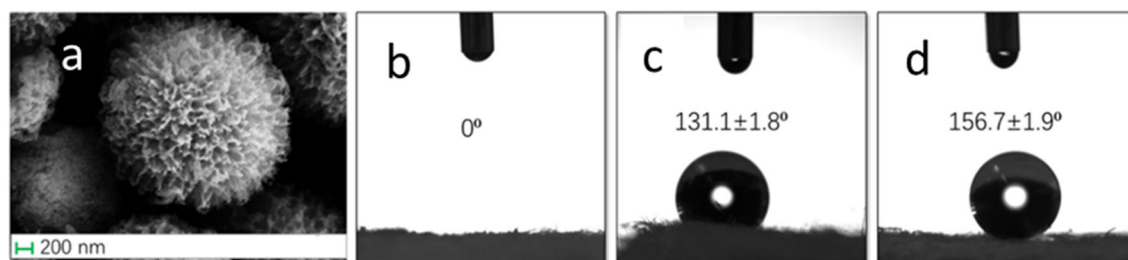


Fig. 15: (a) The SEM image of the flowerlike  $\text{TiO}_2$  particles. (b) Images displaying the water contact angle of (b) pristine cotton, (c) cotton coated with PDMS, and (d) cotton coated with N-doped  $\text{TiO}_2$ /PDMS. Reprinted from: Pakdel, E. et al. Superhydrophobic and photocatalytic self-cleaning cotton fabric using flowerlike N-doped  $\text{TiO}_2$ /PDMS coating. *Cellulose* 2021, 28, 8807–8820,<sup>139</sup> (copyright 2020) with permission from Elsevier

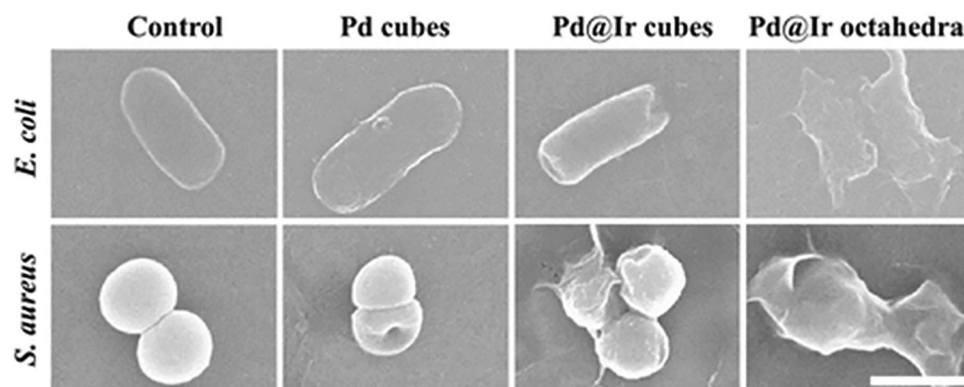


Fig. 16: The SEM images of the bacterial cells treated with Pd-based nanostructures (100  $\mu\text{g}/\text{mL}$ ). Scale bar: 1  $\mu\text{m}$ . Reprinted from: Cai, T. et al. Optimization of antibacterial efficacy of noble-metal-based core–shell nanostructures and effect of natural organic matter. *ACS Nano* 2019, 13, 12,694–12,702,<sup>140</sup> (copyright 2019) with permission from ACS

estingly, the Co– $\text{TiO}_2$  catalyst was active against all bacteria strains tested but not the co-doped catalyst. The Co– $\text{TiO}_2$ –N catalyst was only effective against *L. pneumophila*. The reduced antimicrobial activity was postulated to be associated with fewer Co ions on the catalyst surface in the case of Co– $\text{TiO}_2$ –N. The authors did not observe good antimicrobial activity in visible-light conditions.

Ni-doped  $\text{TiO}_2$  nanospheres were decorated with silver plasmonic nanoparticles (Ni– $\text{TiO}_2$ /Ag) via solgel methods and a photodeposition approach.<sup>143</sup> In contrast to pure  $\text{TiO}_2$  and Ni– $\text{TiO}_2$ , the Ni– $\text{TiO}_2$ /Ag composite photocatalysts showed enhanced visible-light photocatalytic activity toward *E. coli*. This was ascribed to the synergistic effect of Ag decoration and Ni doping, which narrows the band gap, increases the absorption of visible light, and improves the separation efficiency of charge carriers. Also, an antifungal experiment revealed that the composite could disinfect ca. 2.0  $\log_{10}$  cfu·mL<sup>−1</sup> *Fusarium graminearum* macroconidia within 3 h. Electron spin resonance studies verified the roles of  $\cdot\text{O}_2^-$  and  $\cdot\text{OH}$  scavengers during microbial inactivation. This can provide an efficient strategy for developing multifunctional photocatalysts for pathogenic microorganism remediation.

Mutalik et al.<sup>144</sup> prepared  $\text{TiO}_2$ – $\text{FeS}_2$  NPs using hydrothermal methods and annealing the final samples

at 500°C. The materials were incubated with *E. coli* solutions and irradiated for 30 min using a 515 nm long pass filter, destroying all the bacteria. This is a significant result because UV irradiation was cut off in this specific experiment, showing the efficacy of  $\text{TiO}_2$ – $\text{FeS}_2$  NPs under near-infrared conditions.

By combining tourmaline with nanosized nitrogen-doped  $\text{TiO}_2$  particles (T–N– $\text{TiO}_2$ ), a 2-log inactivation of *S. aureus* under 7.25 mW/cm<sup>2</sup> visible-light irradiation was achieved within 3 h. The TEM observations confirmed the damage to cell membranes, and EPR studies indicated that more hydroxyl free radicals generated during photocatalysis allowed for the inactivation of the biocide. Further work, which included more pathogens, showed that an increasing order of time was required for complete inactivation as follows: *S. aureus* < *E. coli* < *M. avium* < *C. albicans*. According to the authors, these results show the highest inactivation efficiency of the tested pathogens in the literature.<sup>145</sup>

Nanoparticles containing noble metals often have dual applications. For example, Cao et al. reported the design and fabrication of  $\text{TiO}_2$  spheres coated with an ultrathin nitrogen-doped carbon (NC) shell and the subsequent loading of Ag nanoparticles. The spherical  $\text{TiO}_2$ @NC/Ag NPs had a narrow bandgap of 2.34 eV and high fluorescence quenching ability. The material

showed a promising bactericidal feature against *E. coli* using low-power LED (6 W) irradiation. Compared to dark conditions, the inhibition rate increased from 59.8% to 87.6%. The composites were further developed as a surface-enhanced Raman scattering (SERS) sensor for rapid detection of the diabetes drug phenformin hydrochloride in human urine with a low detection limit of 5 nM.<sup>146</sup>

Ashfaq et al.<sup>147</sup> co-doped TiO<sub>2</sub> NPs with nitrogen and carbon nitride (C<sub>3</sub>N<sub>4</sub>) using co-precipitation methods (see Fig. 17). The photocatalytic activity was assessed by investigating the degradation of methylene blue and ciprofloxacin. The co-doped NPs showed visible-light photocatalysis and enhanced antibacterial activity against *S. aureus* and *E. coli*.

A visible-light active antibacterial paint containing Ag@TiO<sub>2</sub> NPs was prepared using ultra sonification methods and varying the content of Ag (1–5 wt%) as a photoactive agent.<sup>148</sup> This visible-light active paint was employed for surface disinfection in the visible-light irradiation against Gram-positive and Gram-negative bacteria. The paint was more effective against Gram-negative *E. coli* than Gram-positive *S. aureus*.

Organic polymers with TiO<sub>2</sub> provide interesting opportunities to create films or coatings with antibacterial properties under visible-light conditions. Polyacrylonitrile and its TiO<sub>2</sub> composites were electrospun into nanofibers with a diameter between 10 and 340 nm for photocatalysis and antifouling experiments. The surface produced showed superhydrophobicity with a water contact angle of 154° ± 1 at 120 s. The photocatalytic properties of the polyacrylonitrile-TiO<sub>2</sub>

nanofibers were investigated under a simulated visible-light source of 1000 W/m<sup>2</sup> using methylene blue and compared with polyacrylonitrile nanofibers. After 3 h, 90% of the methylene blue was degraded using polyacrylonitrile-TiO<sub>2</sub> nanofibers, while 55% methylene blue degradation was achieved for the polyacrylonitrile nanofibers. The antimicrobial tests against *E. coli* and *Bacillus* sp. showed that only polyacrylonitrile-TiO<sub>2</sub> under visible light hindered the growth of these bacteria with a more significant effect on the Gram-positive bacterium, *Bacillus* sp.<sup>149</sup>

In another study employing biosynthetic methods, activated carbon/silver/titanium dioxide nanocomposite was successfully synthesized by a hydrothermal method using jasmine flower extract (see Fig. 18 for the SEM images of the particles).<sup>150</sup> The photocatalytic activity under solar light was evaluated by the degradation of methylene blue (MB), and the antibacterial activity was tested against *E. coli* and *S. aureus*. From the characterization, the activated carbon/silver/titanium dioxide nanocomposite has a crystalline, needle-like morphology. Under visible light, the nanocomposite showed 96% maximum degradation efficiency after 120 min. The antibacterial activity was higher than that of commercial TiO<sub>2</sub>.

Antimicrobial coatings of frequent-touch 3-D surfaces like door handles or bed rails in healthcare facilities face several challenges. These coatings require an epoxy binder or a paint mixture containing TiO<sub>2</sub> NPs. It is common knowledge that paints have wear-related issues on frequent-touch surfaces and that the binder would decrease the effective surface area for

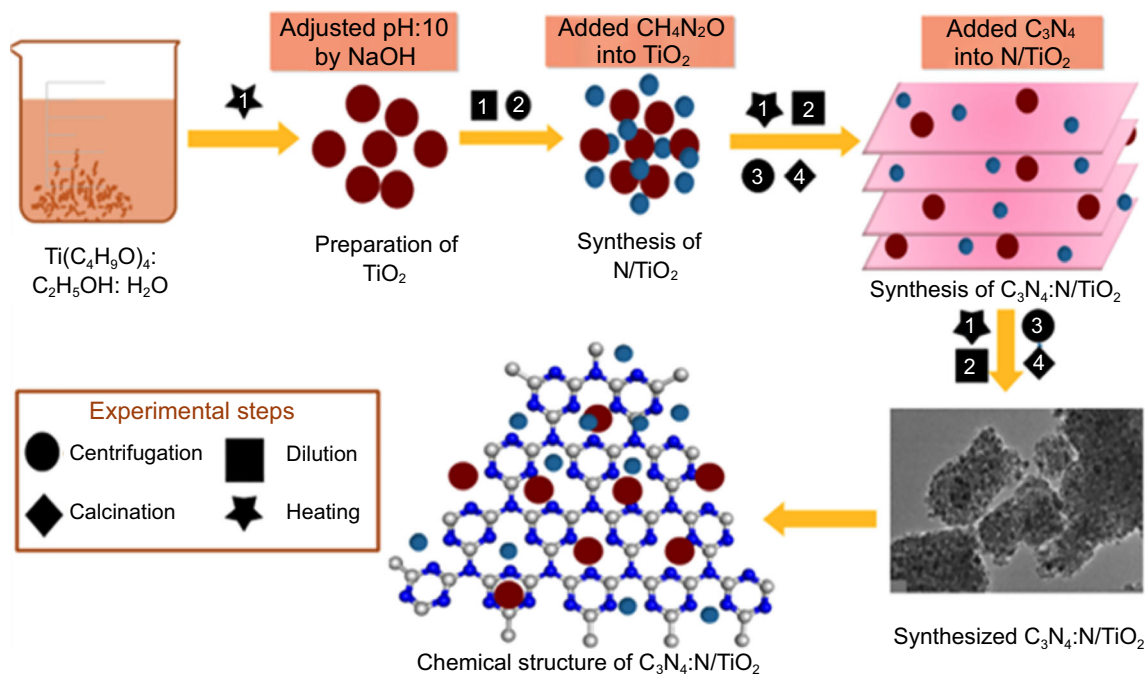
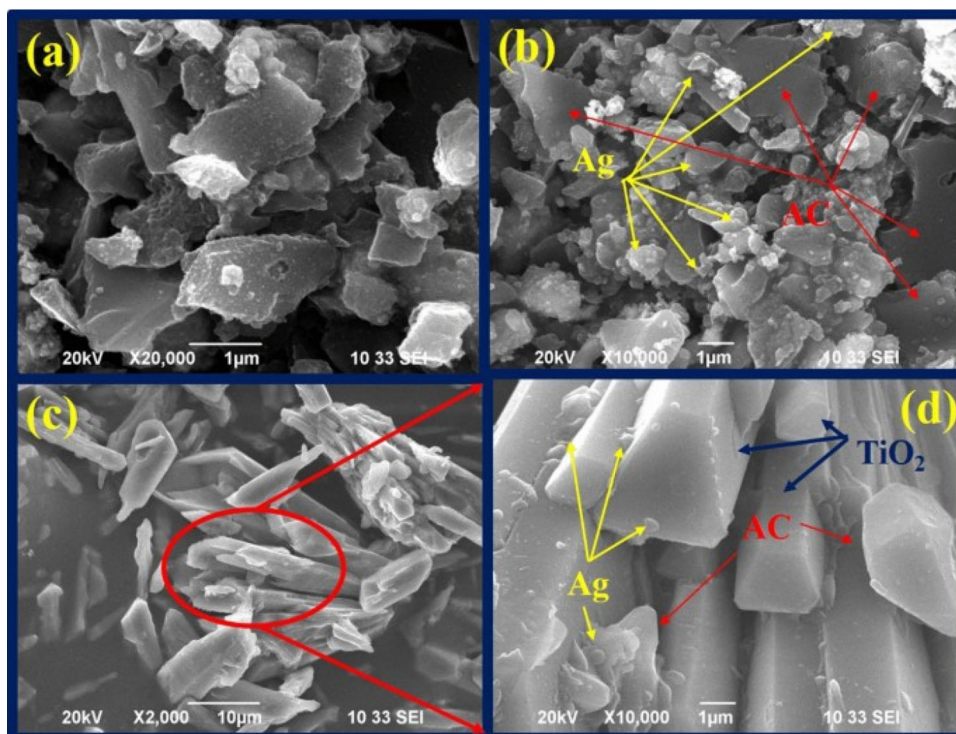


Fig. 17: A schematic illustration of the preparation of C<sub>3</sub>N<sub>4</sub>:N/TiO<sub>2</sub>. Reprinted from: Ashfaq, A. et al. Nitrogen and carbon nitride-doped TiO<sub>2</sub> for multiple catalysis and antimicrobial activity. *Nanoscale Res. Lett.* 2021, 16, 119,<sup>147</sup> (copyright 2021) with permission from Springer Link



**Fig. 18:** The SEM images (a) activated carbon (AC), (b) Ag/AC, (c and d) Ag/AC/TiO<sub>2</sub> nanocomposites. Reprinted from: Aravind, M. et al. Enhanced photocatalytic and biological observations of green synthesized activated carbon, activated carbon doped silver and activated carbon/silver/titanium dioxide nanocomposites. *J. Inorg. Organomet. Polym. Mater.* 2022, 32, 267-279,<sup>150</sup> (copyright 2022) with permission from Springer Link

antimicrobial activity. To overcome this, Krumdieck et al. used the up-scalable metalorganic vapor deposition (pp-MOCVD) process at a high pulsed growth rate to produce a composite of nanostructured anatase, rutile dendrites, and carbon. The coating exhibited strong antimicrobial activity under visible light and in the dark with strong adhesive properties to stainless steel.<sup>151</sup> In a continuation of this study, the antimicrobial properties of this photocatalytic material were tested against a group of microbial species (*E. coli*, *S. aureus*, *P. aeruginosa*, and *S. cerevisiae*) that represents various kinds of pathogens, differ structurally and morphologically, and they show varying responses of resistance to antibiotics and disinfection techniques. Replicates were simultaneously exposed to high-intensity visible light of 2100 lux (450–650 nm), UV light (365 nm), and ambient light (650–750 nm) and kept in the dark for a period of up to 8 h. Compared to the negative control (stainless steel) against *E. coli*, a greater than 3-log reduction was achieved using UV and visible light. A 2-log reduction was observed using ambient light or no light exposure: the positive control, Cu, reduced viability by greater than 4-log to below detection limits. Interestingly, there was no difference in the effectiveness of the material in killing *E. coli* under UV and visible light. Still, significantly greater killing was observed on the photocatalyst under ambient light compared to dark conditions. Similar observations were found for the other microorganisms.

Interestingly, the organisms were also killed in dark conditions, indicating that ROS production is not the only mechanism at play. The authors presented several viable options for the desiccation of cells over time in no light situations. These included the modification of the zeta potential of the cell membranes by direct contact with the NPs leading to increased permeability and their hydrophilic surfaces. The growth of biofilms was prevented, even in dark conditions, which has not been observed for other TiO<sub>2</sub> formulations.<sup>152</sup>

The high cost of noble metals makes it almost impossible to apply them in industrial applications. Therefore, research groups are looking at low-cost earth-abundant minerals with photoic-electrical-chemical properties to modify photocatalysts like TiO<sub>2</sub>. Tourmaline is a borosilicate mineral that can form electric dipoles, has permanent holes, and undergoes spontaneous polarization. A comparison of the properties against *S. aureus*, *E. coli*, and *M. avium* of nitrogen-doped titanium oxide NPs (N-TiO<sub>2</sub>) and tourmaline-nitrogen-co-doped titanium oxide NPs (T-N-TiO<sub>2</sub>) under visible light irradiation produced exciting results (see Fig. 19 for the comparative graph of survival). The visible-light inactivation of *S. aureus* with T-N-TiO<sub>2</sub> was an hour faster than that obtained for N-TiO<sub>2</sub> (4 h). The authors used TEM to illustrate the damage to the cell membranes (see Figs. 19b and 19c for the TEM images) and electron paramagnetic resonance to show that T-N-TiO<sub>2</sub> generated more

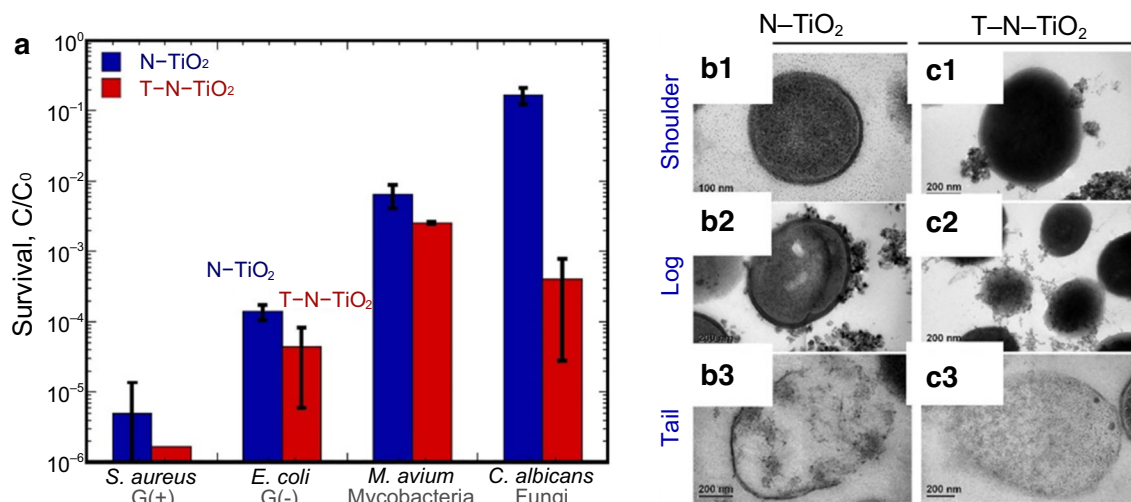


**Fig. 19: (a)** Comparative graph showing the survival of the different cells incubated with N-TiO<sub>2</sub> and T-N-TiO<sub>2</sub> under visible-light irradiation. TEM images of *S. aureus* incubated with N-TiO<sub>2</sub> and T-N-TiO<sub>2</sub> under visible-light irradiation 0 h, 2 h, and 24 h with (a1–a3) N-TiO<sub>2</sub> and (b1–b3) T-N-TiO<sub>2</sub> under visible-light irradiation. Reprinted from: Tzeng, J.-H. et al. Inactivation of pathogens by visible-light photocatalysis with nitrogen-doped TiO<sub>2</sub> and tourmaline-nitrogen co-doped TiO<sub>2</sub>. *Sep. Purif. Technol.* 2021, 274, 118,979,<sup>145</sup> (copyright 2021) with permission from Elsevier

hydroxyl radicals and thus better inactivation. According to the authors, this photocatalyst produced the highest yet reported inactivation results compared to the available literature.<sup>145</sup>

Another active area of research is the incorporation of fluorine into TiO<sub>2</sub> coatings to increase the production of ROS. An example of this is in the study of Park et al. They suspended nanoparticles in a PEG solution and then spread, dried, and calcified the mixture onto glass slides before immersing it in a NaF solution to obtain a TiO<sub>2</sub>-F coating. They aimed to produce a photocatalyst that would be effective under typical office conditions with fluorescent lighting: 3.5 μW/cm<sup>2</sup> of UVA at a wavelength of ~365 nm. The coatings were then evaluated against human norovirus, bacteriophage MS2, feline calicivirus (FCV), and murine norovirus. Exposure to their light source for 80 min on pristine TiO<sub>2</sub> film and the newly fabricated F-TiO<sub>2</sub> surfaces showed much faster kinetics for the fluorinated surfaces and obtained approximately 4 times faster inactivation performance. While most modern offices use fluorescent lights, the authors mentioned that this TiO<sub>2</sub>-F coating would not be effective in normal light conditions. However, adding another dopant might be something to consider for future research.<sup>153</sup>

It is worth mentioning that a TiO<sub>2</sub> co-doped with nitrogen and bismuth has been coated onto medical implants for their visible-light-induced antibacterial activity.<sup>154</sup> The electrochemical anodic oxidation of titanium metal results in the formation of titanium nanotubes (see the SEM image in Fig. 20).<sup>155</sup> This has been reported for its antimicrobial and antibiofilm properties under UV irradiation when covering medical implants and devices.<sup>156</sup>

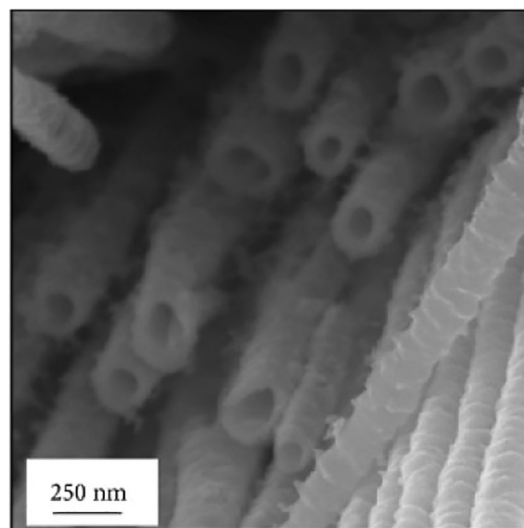


**Fig. 20: The SEM image of the TiO<sub>2</sub> nanotubes.** Reprinted from: Zhang, Q. et al. Anodic oxidation synthesis of one-dimensional TiO<sub>2</sub> nanostructures for photocatalytic and field emission properties. *J. Nanomater.* 2014, 2014, 1–14,<sup>155</sup> (copyright 2014) with permission from Hindawi

While not used as a coating, the synthesis of red phosphorus/titanium oxide (TiO<sub>2</sub>@RP) nanofibers developed for effective water disinfection needs mentioning. The catalyst killed *E. coli* and *S. aureus* (7-log CFU mL<sup>-1</sup>) within 25 min and 30 min, respectively, under white LED lighting. The generation of •OH and •O<sub>2</sub><sup>-</sup> radicals was confirmed by electron paramagnetic resonance. They added isopropanol scavengers for •OH, Cr(VI) for electrons (e<sup>-</sup>), sodium oxalate for holes (h<sup>+</sup>), 4-hydroxy-2,2,6,6-tetramethylpiperidinyloxy (TEMPO) for •O<sub>2</sub><sup>-</sup>, and catalase for H<sub>2</sub>O<sub>2</sub>,

respectively, to determine the primary reactive species during the photocatalysis. The results showed that  $\text{H}^+$ ,  $\bullet\text{O}_2^-$ , and  $\text{H}_2\text{O}_2$  were the critical species for photocatalytic antibacterial properties.<sup>157</sup>

### Other interesting innovations

While not developed for visible-light photocatalysis, the very recent work of Song et al.<sup>158</sup> should be noticed for further development (see Fig. 21). They used electrospinning methods to develop a reusable hydrophilic self-cleaning film with a bilayer structure that combined the mechanical strength of acrylonitrile–butadiene–styrene (ABS) resins with poly(vinyl alcohol) (PVA), showing the concept of bilayering the self-cleaning films. An ABS/ $\text{TiO}_2$  fiber film on the substrate layer provided self-cleaning ability under UV light. The authors proved the reusability by applying the same films on different surfaces and observing the degradation of methylene blue. The critical aspect of this work is twofold. Firstly, such films could allow for the fabrication of medical equipment that can be recycled, thus reducing costs. Secondly, it provides opportunities for further development of photocatalysis under visible light using doping techniques.

In another project, non-decomposable plastic was replaced with polylactic acid (PLA), a biodegradable aliphatic polyester stationary phase in composite films embedded with a  $\text{TiO}_2$  photocatalyst to mitigate indoor air pollution.<sup>159</sup> Compared to other biopolymers, PLA has excellent properties in terms of high melting point, crystallinity, and rigidity. By incorporating  $\text{TiO}_2$ -anatase into PLA using the blown film method with a twin-screw extruder (5, 10 and 15% (wt/wt)), a prototype air purifier reactor model was developed to test the  $\text{TiO}_2$ /PLA composite films

against benzene degradation under UV light. The 5% wt sample showed the best photocatalytic activity and removed 44% of benzene in 15 h under simulated indoor air conditions. This work creates opportunities for co-doping, which could lead to the development of air filters which do not necessarily need UV light activation.

### Environmentally friendly synthesis of $\text{TiO}_2$

Since  $\text{TiO}_2$  NPs are considered environmentally safe, using ecologically friendly synthetic procedures to prepare these NPs would make them even more attractive for various applications. Several different biosynthesis routes can be followed to prepare  $\text{TiO}_2$  as opposed to the traditional sol-gel process, such as microbial and photosynthesis. In this review, we will only focus on photosynthesis seeing it can be used for large-scale production of  $\text{TiO}_2$ .

It has been reported that phytochemicals (plant extract) assist in nanoparticle formation. As mentioned earlier, jasmine flower extract has been used to synthesize activated carbon/silver/titanium dioxide nanocomposites.<sup>150</sup> For example, sonication of lemongrass extract and the Ti-precursor (titanium(IV) isopropoxide), followed by calcination at  $550^\circ\text{C}$ , resulted in the formation of the anatase phase with an average size of *ca.* 12.3 nm.<sup>160</sup> These were incorporated into the paint for anticorrosive, antibacterial, and self-cleaning properties. Rutile  $\text{TiO}_2$  NPs were prepared from a low-temperature biodegradable process using agricultural waste (extracts of *Annona squamosa* fruit peel).<sup>161</sup> The spherical particle had an average size of 23 nm.

Vembu et al.<sup>162</sup> prepared  $\text{TiO}_2$  NPs from *Pisonia grandis* (grand devil's-claws, a species of the Bougainvillea family) extract showed excellent anti-



Fig. 21: Photographic illustration of the concept of bilayer the  $\text{TiO}_2$  self-cleaning films. Reprinted from: Song, K. et al. Electro-spray deposited  $\text{TiO}_2$  bilayer films and their recyclable photocatalytic self-cleaning strategy. *Sci. Rep.* 2022, 12, 1582,<sup>158</sup> (copyright 2022) with permission from Springer Nature

crobial and cytotoxic activity against SaOS2 cancer cell lines.

In a low-cost procedure using the extract of the bitter herbal plant, *Andrographis paniculata*, 23 nm sized TiO<sub>2</sub> NPs were prepared, which showed antioxidant and antidiabetic activity.<sup>163</sup> Other plant extracts that can be used to phytosynthesize TiO<sub>2</sub> NPs include *Azadirachta indica* (Neem) leaf,<sup>164</sup> *Diospyros ebenum* leaf extract,<sup>165</sup> extracts from the leaves, seeds, and seed shells of the kola nut tree (*Cola nitida*),<sup>166</sup> *Enterolobium saman* bark extract,<sup>167</sup> and pomegranate rind.<sup>168</sup>

It has been reported that nanoparticles prepared via phytosynthesis of herbal-derived material results in increased biocompatibility and biodegradability.<sup>117</sup> Additionally, using a mixture of two plant extracts to prepare NPs can result in the combined effect of suitable biocompatibility and synergistic antibacterial effect. This could potentially be a practical approach for a green preparation of TiO<sub>2</sub> and other metal oxide NPs with improved properties.

### Final thoughts and future prospects

The recent COVID-19 pandemic instilled a new drive toward developing antimicrobial and antiviral coatings, utilizing many different technologies and materials. Of these, photocatalysis using TiO<sub>2</sub> is one of the most exciting propositions. However, normal disinfection processes should not be neglected despite not having permanent effects. Instead, these practices should run in synergy with anti-MoV coatings and paints. The potential application of these coatings and paints in real-life situations is subjected to various challenges, but this is also where future opportunities will be found.

Firstly, the risk of NPs leaching from these materials has been discussed on various platforms. However, very few articles we reviewed investigated this aspect over time or in different environments that mimic real-life situations. It was also suggested that these technologies be adequately tested using standardized methods and field studies before being utilized in medical or other facilities. However, this is doubtful because of the pressure from market needs. Another problem is that some materials are efficient against specific pathogens but not against others. Finding a broad-spectrum coating will be a struggle, highlighting the requirement of standard disinfection methods working in synergy with new technologies. The biodegradability of materials and coatings should also be evaluated before implementation. This is rarely done. For example, the outer and inner linings of female sanitary napkins take 500 years to biodegrade, creating thousands of tons of chemical waste each year.<sup>169</sup> Indeed, the world does not need a similar example. Therefore green syntheses, using low-energy methods and scrupulous testing methods, can make

this a success story. The use of visible light to combat MoVs effectively is not a distinct probability anymore but nearly a reality. We now need innovative, responsible research with an intent to get to real-life solutions instead of good laboratory results that look good on yet another published article.

**Acknowledgments** The University of the Free State, Bloemfontein, South Africa, is also acknowledged for financial support.

**Funding** Funding was provided by Universiteit van die Vrystaat.

**Conflict of interest** The authors have no conflicts of interest to declare. All co-authors have seen and agree with the manuscript's contents and there is no financial interest to report.

### References

1. Khan, HA, Baig, FK, Mehboob, R, "Nosocomial Infections: Epidemiology, Prevention, Control and Surveillance." *Asian Pac. J. Trop. Biomed.*, **7** 478–482. <https://doi.org/10.1016/j.apjtb.2017.01.019> (2017)
2. Weber, DJ, Anderson, D, Rutala, WA, "The Role of the Surface Environment in Healthcare-Associated Infections." *Curr. Opin. Infect. Dis.*, **26** 338–344. <https://doi.org/10.1097/QCO.0b013e3283630f04> (2013)
3. Kramer, A, Schwebke, I, Kampf, G, "How Long do Nosocomial Pathogens Persist on Inanimate Surfaces? A Systematic Review." *BMC Infect. Dis.*, **6** 130. <https://doi.org/10.1186/1471-2334-6-130> (2006)
4. van Doremalen, N, Bushmaker, T, Morris, DH, Holbrook, MG, Gamble, A, Williamson, BN, Tamin, A, Harcourt, JL, Thornburg, NJ, Gerber, SI, Lloyd-Smith, JO, de Wit, E, Munster, VJ, "Aerosol and Surface Stability of SARS-CoV-2 as Compared with SARS-CoV-1." *N. Engl. J. Med.*, **382** 1564–1567. <https://doi.org/10.1056/NEJMc2004973> (2020)
5. Kramer, A, Assadian, O, "Survival of Microorganisms on Inanimate Surfaces." In: *Use Biocidal Surfaces Reduction of Healthcare Acquired Infections*, pp. 7–26. Springer International Publishing, Cham (2014)
6. Kampf, G, Todt, D, Pfaender, S, Steinmann, E, "Persistence of Coronaviruses on Inanimate Surfaces and Their Inactivation with Biocidal Agents." *J. Hosp. Infect.*, **104** 246–251. <https://doi.org/10.1016/j.jhin.2020.01.022> (2020)
7. Hamilton, KA, Hamilton, MT, Johnson, W, Jjemba, P, Bukhari, Z, LeChevallier, M, Haas, CN, "Health Risks from Exposure to *Legionella* in Reclaimed Water Aerosols: Toilet Flushing, Spray Irrigation, and Cooling Towers." *Water Res.*, **134** 261–279. <https://doi.org/10.1016/j.watres.2017.12.022> (2018)
8. Wang, Y, Du, H, Xie, M, Ma, G, Yang, W, Hu, Q, Pei, F, "Characterization of the Physical Properties and Biological Activity of Chitosan Films Grafted with Gallic Acid and Caffeic Acid: A Comparison Study." *Food Packag. Shelf Life.*, **22** 100401. <https://doi.org/10.1016/j.fpsl.2019.100401> (2019)

9. Jung, Y, Jang, H, Guo, M, Gao, J, Matthews, KR, “Sanitizer Efficacy in Preventing Cross-Contamination of Heads of Lettuce During Retail Crisping.” *Food Microbiol.*, **64** 179–185. <https://doi.org/10.1016/j.fm.2017.01.005> (2017)
10. Brogden, KA, Guthmiller, JM, Taylor, CE, “Human Polymicrobial Infections.” *Lancet*, **365** 253–255. [https://doi.org/10.1016/S0140-6736\(05\)17745-9](https://doi.org/10.1016/S0140-6736(05)17745-9) (2005)
11. Levin-Reisman, I, Ronin, I, Gefen, O, Braniss, I, Shoshan, N, Balaban, NQ, “Antibiotic Tolerance Facilitates the Evolution of Resistance.” *Science*, **355** (6327) 826–830. <https://doi.org/10.1126/science.aaj2191> (2017)
12. Habimana, O, Heir, E, Langsrud, S, Asli, AW, Mørseth, T, “Enhanced Surface Colonization by *Escherichia coli* O157:H7 in Biofilms Formed by an *Acinetobacter calcoaceticus* Isolate from Meat-Processing Environments.” *Appl. Environ. Microbiol.*, **76** 4557–4559. <https://doi.org/10.1128/AEM.02707-09> (2010)
13. Burmølle, M, Webb, JS, Rao, D, Hansen, LH, Sørensen, SJ, Kjelleberg, S, “Enhanced Biofilm Formation and Increased Resistance to Antimicrobial Agents and Bacterial Invasion Are Caused by Synergistic Interactions in Multispecies Biofilms.” *Appl. Environ. Microbiol.*, **72** 3916–3923. <https://doi.org/10.1128/AEM.03022-05> (2006)
14. Dang, H, Lovell, CR, “Microbial Surface Colonization and Biofilm Development in Marine Environments.” *Microbiol. Mol. Biol. Rev.*, **80** 91–138. <https://doi.org/10.1128/MMBR.00037-15> (2016)
15. Grinberg, M, Orevi, T, Kashtan, N, “Bacterial Surface Colonization, Preferential Attachment and Fitness Under Periodic Stress.” *PLOS Comput. Biol.*, **15** e1006815. <https://doi.org/10.1371/journal.pcbi.1006815> (2019)
16. Ledwoch, K, Dancer, SJ, Otter, JA, Kerr, K, Roposte, D, Maillard, J-Y, “How Dirty is Your QWERTY? The Risk of Healthcare Pathogen Transmission from Computer Keyboards.” *J. Hosp. Infect.*, **112** 31–36. <https://doi.org/10.1016/j.jhin.2021.02.021> (2021)
17. Ledwoch, K, Dancer, SJ, Otter, JA, Kerr, K, Roposte, D, Rushton, L, Weiser, R, Mahenthalingam, E, Muir, DD, Maillard, J-Y, “Beware Biofilm! Dry Biofilms Containing Bacterial Pathogens on Multiple Healthcare Surfaces; a Multi-Centre Study.” *J. Hosp. Infect.*, **100** e47–e56. <https://doi.org/10.1016/j.jhin.2018.06.028> (2018)
18. Amaeze, N, Akinbobola, A, Chukwuemeka, V, Abalkhaila, A, Ramage, G, Kean, R, Staines, H, Williams, C, Mackay, W, “Development of a High Throughput and Low Cost Model for the Study of Semi-Dry Biofilms.” *Biofouling*, **36** 403–415. <https://doi.org/10.1080/08927014.2020.1766030> (2020)
19. Ponde, NO, Lortal, L, Ramage, G, Naglik, JR, Richardson, JP, “*Candida albicans* Biofilms and Polymicrobial Interactions.” *Crit. Rev. Microbiol.*, **47** 91–111. <https://doi.org/10.1080/1040841X.2020.1843400> (2021)
20. Tolker-Nielsen, T, “Biofilm Development.” *Microbiol. Spectr.*, **3** (2) 3–2. <https://doi.org/10.1128/microbiolspec.MB-0001-2014> (2015)
21. Achinas, S, Charalampogiannis, N, Euverink, GJW, “A Brief Recap of Microbial Adhesion and Biofilms.” *Appl. Sci.*, **9** 2801. <https://doi.org/10.3390/app9142801> (2019)
22. Berne, C, Ellison, CK, Ducret, A, Brun, YV, “Bacterial Adhesion at the Single-Cell Level.” *Nat. Rev. Microbiol.*, **16** 616–627. <https://doi.org/10.1038/s41579-018-0057-5> (2018)
23. Casagrande Pierantoni, D, Corte, L, Casadevall, A, Robert, V, Cardinali, G, Tascini, C, “How Does Temperature Trigger Biofilm Adhesion And Growth in *Candida albicans* and Two Non-*Candida albicans* *Candida* Species?” *Myco*, **64** 1412–1421. <https://doi.org/10.1111/myc.13291> (2021)
24. Talebian, S, Wallace, GG, Schroeder, A, Stellacci, F, Conde, J, “Nanotechnology-Based Disinfectants and Sensors for SARS-CoV-2.” *Nat. Nanotechnol.*, **15** 618–621. <https://doi.org/10.1038/s41565-020-0751-0> (2020)
25. Vasickova, P, Pavlik, I, Verani, M, Carducci, A, “Issues Concerning Survival of Viruses on Surfaces.” *Food Environ. Virol.*, **2** 24–34. <https://doi.org/10.1007/s12560-010-9025-6> (2010)
26. Birkett, M, Dover, L, Cherian Lukose, C, Wasy Zia, A, Tambuwala, MM, Serrano-Aroca, Á, “Recent Advances in Metal-Based Antimicrobial Coatings for High-Touch Surfaces.” *Int. J. Mol. Sci.*, **23** 1162. <https://doi.org/10.3390/ijm23031162> (2022)
27. Prestinaci, F, Pezzotti, P, Pantosti, A, “Antimicrobial Resistance: A Global Multifaceted Phenomenon.” *Pathog. Glob Health*, **109** 309–318. <https://doi.org/10.1179/2047773215Y.0000000030> (2015)
28. Humphreys, G, Fleck, F, “United Nations Meeting on Antimicrobial Resistance.” *Bull. World Health Org.*, **94** 638–639. <https://doi.org/10.2471/BLT.16.020916> (2016)
29. Riddell, S, Goldie, S, Hill, A, Eagles, D, Drew, TW, “The Effect of Temperature on Persistence of SARS-CoV-2 on Common Surfaces.” *Virol. J.*, **17** 145. <https://doi.org/10.1186/s12985-020-01418-7> (2020)
30. Kumaravel, V, Nair, KM, Mathew, S, Bartlett, J, Kennedy, JE, Manning, HG, Whelan, BJ, Leyland, NS, Pillai, SC, “Antimicrobial TiO<sub>2</sub> Nanocomposite Coatings for Surfaces, Dental and Orthopaedic Implants.” *Chem. Eng. J.*, **416** 129071. <https://doi.org/10.1016/j.cej.2021.129071> (2021)
31. Wang, M, Duday, D, Scolan, E, Perbal, S, Prato, M, Lasseur, C, Holyńska, M, “Antimicrobial Surfaces for Applications on Confined Inhabited Space Stations.” *Adv. Mater. Interfaces*, **8** 2100118. <https://doi.org/10.1002/admi.202100118> (2021)
32. Sun, Z, Ostrikov, KK, “Future Antiviral Surfaces: Lessons From COVID-19 Pandemic.” *Sustain. Mater. Technol.*, **25** e00203. <https://doi.org/10.1016/j.susmat.2020.e00203> (2020)
33. Ghedini, E, Pizzolato, M, Longo, L, Menegazzo, F, Zanardo, D, Signoretto, M, “Which Are the Main Surface Disinfection Approaches at the Time of SARS-CoV-2?” *Front. Chem. Eng.*, **2** 589202. <https://doi.org/10.3389/fceng.2020.589202> (2021)
34. Khaiboullina, S, Uppal, T, Dhabarde, N, Subramanian, VR, Verma, SC, “Inactivation of Human Coronavirus by Titania Nanoparticle Coatings and UVC Radiation: Throwing Light on SARS-CoV-2.” *Viruses*, **13** 19. <https://doi.org/10.3390/v13010019> (2020)
35. Hoffmann, MR, Martin, ST, Choi, W, Bahnemann, DW, “Environmental Applications of Semiconductor Photocatalysis.” *Chem. Rev.*, **95** 69–96. <https://doi.org/10.1021/cr00033a004> (1995)
36. Allahverdiyev, AM, Abamor, ES, Bagirova, M, Rafailovich, M, “Antimicrobial Effects of TiO<sub>2</sub> and Ag<sub>2</sub>O Nanoparticles Against Drug-Resistant Bacteria and *Leishmania* Parasites.” *Future Microbiol.*, **6** 933–940. <https://doi.org/10.2217/fmb.11.78> (2011)
37. De Filipo, G, Palermo, AM, Rachiele, F, Nicoletta, FP, “Preventing Fungal Growth in Wood by Titanium Dioxide Nanoparticles.” *Int. Biodeterior. Biodegr.*, **85** 217–222. <https://doi.org/10.1016/j.ibiod.2013.07.007> (2013)
38. Ganguli, P, Chaudhuri, S, “Nanomaterials in Antimicrobial Paints and Coatings to Prevent Biodegradation of Man-Made Surfaces: A Review.” *Mater. Today Proc.*, **45** 3769–3777. <https://doi.org/10.1016/j.matpr.2021.01.275> (2021)

39. Fisher, MB, Keane, DA, Fernández-Ibáñez, P, Colreavy, J, Hinder, SJ, McGuigan, KG, Pillai, SC, “Nitrogen and Copper Doped Solar Light Active TiO<sub>2</sub> Photocatalysts for Water Decontamination.” *Appl. Catal. B Environ.*, **130–131** 8–13. <https://doi.org/10.1016/j.apcatb.2012.10.013> (2013)
40. De Pasquale, I, Lo Porto, C, Dell’Edera, M, Curri, ML, Comparelli, R, “TiO<sub>2</sub>-Based Nanomaterials Assisted Photocatalytic Treatment for Virus Inactivation: Perspectives and Applications.” *Curr. Opin. Chem. Eng.*, **34** 100716. <https://doi.org/10.1016/j.coche.2021.100716> (2021)
41. Huang, Z, Maness, P-C, Blake, DM, Wolfrum, EJ, Smolinski, SL, Jacoby, WA, “Bactericidal Mode of Titanium Dioxide Photocatalysis.” *J. Photochem. Photobiol. A Chem.*, **130** 163–170. [https://doi.org/10.1016/S1010-6030\(99\)00205-1](https://doi.org/10.1016/S1010-6030(99)00205-1) (2000)
42. Munafò, P, Goffredo, GB, Quagliarini, E, “TiO<sub>2</sub>-Based Nanocoatings for Preserving Architectural Stone Surfaces: An Overview.” *Constr. Build. Mater.*, **84** 201–218. <https://doi.org/10.1016/j.conbuildmat.2015.02.083> (2015)
43. Cho, M, Chung, H, Choi, W, Yoon, J, “Linear Correlation Between Inactivation of *E. coli* and OH Radical Concentration in TiO<sub>2</sub> Photocatalytic Disinfection.” *Water Res.*, **38** 1069–1077. <https://doi.org/10.1016/j.watres.2003.10.029> (2004)
44. Padmanabhan, NT, John, H, “Titanium Dioxide Based Self-Cleaning Smart Surfaces: A Short Review.” *J. Environ. Chem. Eng.*, **8** 104211. <https://doi.org/10.1016/j.jece.2020.10.4211> (2020)
45. Becerra, J, Zaderenko, AP, Sayagués, MJ, Ortiz, R, Ortiz, P, “Synergy Achieved in Silver-TiO<sub>2</sub> Nanocomposites for the Inhibition of Biofouling on Limestone.” *Build. Environ.*, **141** 80–90. <https://doi.org/10.1016/j.buildenv.2018.05.020> (2018)
46. Dalawai, SP, Saad Aly, MA, Latthe, SS, Xing, R, Sutar, RS, Nagappan, S, Ha, C-S, Kumar Sadasivuni, K, Liu, S, “Recent Advances in Durability of Superhydrophobic Self-cleaning Technology: A Critical Review.” *Prog. Org. Coat.*, **138** 105381. <https://doi.org/10.1016/j.porgcoat.2019.105381> (2020)
47. Herrmann, J-M, “Heterogeneous Photocatalysis: Fundamentals and Applications to the Removal of Various Types of Aqueous Pollutants.” *Catal. Today.*, **53** 115–129. [https://doi.org/10.1016/S0920-5861\(99\)00107-8](https://doi.org/10.1016/S0920-5861(99)00107-8) (1999)
48. Liu, L, Bai, H, Liu, J, Sun, DD, “Multifunctional Graphene Oxide-TiO<sub>2</sub>-Ag Nanocomposites for High Performance Water Disinfection and Decontamination Under Solar Irradiation.” *J. Hazard. Mater.*, **261** 214–223. <https://doi.org/10.1016/j.jhazmat.2013.07.034> (2013)
49. Mogal, SI, Mishra, M, Gandhi, VG, Tayade, RJ, “Metal Doped Titanium Dioxide: Synthesis and Effect of Metal Ions on Physico-Chemical and Photocatalytic Properties.” *Mater. Sci. Forum.*, **734** 364–378. <https://doi.org/10.4028/www.scientific.net/MSF.734.364> (2012)
50. Zhang, H, Wang, X, Li, N, Xia, J, Meng, Q, Ding, J, Lu, J, “Synthesis and Characterization of TiO<sub>2</sub>/Graphene Oxide Nanocomposites for Photoreduction of Heavy Metal Ions in Reverse Osmosis Concentrate.” *RSC Adv.*, **8** 34241–34251. <https://doi.org/10.1039/C8RA06681G> (2018)
51. Jiang, D, Otitoju, TA, Ouyang, Y, Shoparwe, NF, Wang, S, Zhang, A, Li, S, “A Review on Metal Ions Modified TiO<sub>2</sub> for Photocatalytic Degradation of Organic Pollutants.” *Catalysts*, **11** 1039. <https://doi.org/10.3390/catal11091039> (2021)
52. Qiu, X, Miyauchi, M, Sunada, K, Minoshima, M, Liu, M, Lu, Y, Li, D, Shimodaira, Y, Hosogi, Y, Kuroda, Y, Hashimoto, K, “Hybrid Cu<sub>x</sub>O/TiO<sub>2</sub> Nanocomposites As Risk-Reduction Materials in Indoor Environments.” *ACS Nano*, **6** 1609–1618. <https://doi.org/10.1021/nn2045888> (2012)
53. Berninghausen, LK, Osterhoff, G, Langer, S, Kohler, LH, “Scar Quality Examination Comparing Titanium-Coated Suture Material and Non-Coated Suture Material on Flap Donor Sites in Reconstructive Surgery.” *BMC Surg.*, **20** 268. <https://doi.org/10.1186/s12893-020-00932-3> (2020)
54. Rezk, AI, Lee, JY, Son, BC, Park, CH, Kim, CS, “Bi-Layered Nanofibers Membrane Loaded with Titanium Oxide and Tetracycline as Controlled Drug Delivery System for Wound Dressing Applications.” *Polymers*, **11** (10) 1602. <https://doi.org/10.3390/polym11101602> (2019)
55. Deb, A, Vimala, R, “Biofilm Formation by Pseudomonas Species Onto Graphene Oxide-TiO<sub>2</sub> Nanocomposite-Coated Catheters: In Vitro Analysis.” *Int. J. Nanosci.*, **17** 1760014. <https://doi.org/10.1142/S0219581X17600146> (2018)
56. Sekiguchi, Y, Yao, Y, Ohko, Y, Tanaka, K, Ishido, T, Fujishima, A, Kubota, Y, “Self-Sterilizing Catheters with Titanium Dioxide Photocatalyst Thin Films for Clean Intermittent Catheterization: Basis and Study of Clinical Use.” *Int. J. Urol.*, **14** 426–430. <https://doi.org/10.1111/j.1442-2042.2007.01743.x> (2007)
57. Chung, C-J, Lin, H-I, Tsou, H-K, Shi, Z-Y, He, J-L, “An Antimicrobial TiO<sub>2</sub> Coating for Reducing Hospital-acquired Infection.” *J Biomed. Mater. Res. Part B Appl. Biomater.*, **85B** 220–224. <https://doi.org/10.1002/jbm.b.30939> (2008)
58. Tsou, H, Hsieh, P, “Anticorrosive, Antimicrobial, and Bioactive Titanium Dioxide Coating for Surface-modified Purpose on Biomedical Material.” In: *Application of Titanium Dioxide*. InTech (2017)
59. Jašková, V, Hochmannová, L, Vyřasová, J, “TiO<sub>2</sub> and ZnO Nanoparticles in Photocatalytic and Hygienic Coatings.” *Int. J. Photoenergy*, **2013** 1–6. <https://doi.org/10.1155/2013/795060> (2013)
60. Xia, W, Grandfield, K, Hoess, A, Ballo, A, Cai, Y, Engqvist, H, “Mesoporous Titanium Dioxide Coating for Metallic Implants.” *J. Biomed. Mater. Res. Part B Appl. Biomater.*, **100B** 82–93. <https://doi.org/10.1002/jbm.b.31925> (2012)
61. Della Valle, C, Visai, L, Santin, M, Cigada, A, Candiani, G, Pezzoli, D, Arciola, CR, Imbriani, M, Chiesa, R, “A Novel Antibacterial Modification Treatment of Titanium Capable to Improve Osseointegration.” *Int. J. Artif. Organs*, **35** 864–875. <https://doi.org/10.5301/ijao.5000161> (2012)
62. Yang, X, Chung, E, Johnston, I, Ren, G, Cheong, Y-K, “Exploitation of Antimicrobial Nanoparticles and Their Applications in Biomedical Engineering.” *Appl. Sci.*, **11** 4520. <https://doi.org/10.3390/app11104520> (2021)
63. Vijayaraghavan, R, “Chemical Manipulation of Oxygen Vacancy and Antibacterial Activity in ZnO.” *Mater. Sci. Eng. C*, **77** 1027–1034. <https://doi.org/10.1016/j.msec.2017.03.280> (2017)
64. Shi, T, Hou, X, Guo, S, Zhang, L, Wei, C, Peng, T, Hu, X, “Nanohole-Boosted Electron Transport Between Nanomaterials and Bacteria as a Concept for Nano-Bio Interactions.” *Nat. Commun.*, **12** 493. <https://doi.org/10.1038/s41467-020-20547-9> (2021)
65. Pal, S, Tak, YK, Song, JM, “Does the Antibacterial Activity of Silver Nanoparticles Depend on the Shape of the Nanoparticle? A Study of the Gram-Negative Bacterium *Escherichia coli*.” *Appl. Environ. Microbiol.*, **73** 1712–1720. <https://doi.org/10.1128/AEM.02218-06> (2007)
66. Ren, J, Wang, W, Sun, S, Zhang, L, Wang, L, Chang, J, “Crystallography Facet-Dependent Antibacterial Activity:

- The Case of Cu<sub>2</sub>O.” *Ind. Eng. Chem. Res.*, **50** 10366–10369. <https://doi.org/10.1021/ie2005466> (2011)
67. Rakowska, PD, Tiddia, M, Faruqui, N, Bankier, C, Pei, Y, Pollard, AJ, Zhang, J, Gilmore, IS, “Antiviral Surfaces and Coatings and Their Mechanisms of Action.” *Commun. Mater.*, **2** 53. <https://doi.org/10.1038/s43246-021-00153-y> (2021)
  68. Ziental, D, Czarczynska-Goslinska, B, Mlynarczyk, DT, Glowacka-Sobotta, A, Stanis, B, Goslinski, T, Sobotta, L, “Titanium Dioxide Nanoparticles: Prospects and Applications in Medicine.” *Nanomaterials*, **10** 387. <https://doi.org/10.3390/nano10020387> (2020)
  69. Chen, MC, Koh, PW, Ponnusamy, VK, Lee, SL, “Titanium Dioxide and Other Nanomaterials Based Antimicrobial Additives in Functional Paints and Coatings: Review.” *Prog. Org. Coat.*, **163** 106660. <https://doi.org/10.1016/j.porgcoat.2021.106660> (2022)
  70. Giampiccolo, A, Tobaldi, DM, Jones, E, Labrincha, JA, Kurchania, R, Ansell, MP, Ball, RJ, “UV/Visible Sol Gel W-TiO<sub>2</sub> Photocatalytic Coatings for Interior Building Surfaces.” *Build. Environ.*, **205** 108203. <https://doi.org/10.1016/j.buildenv.2021.108203> (2021)
  71. Verma, J, Bhattacharya, A, “Development of Coating Formulation with Silica–Titania Core–Shell Nanoparticles Against Pathogenic Fungus.” *R. Soc. Open Sci.*, **5** 180633. <https://doi.org/10.1098/rsos.180633> (2018)
  72. Lettieri, M, Colangiuli, D, Masieri, M, Calia, A, “Field Performances of Nanosized TiO<sub>2</sub> Coated Limestone for a Self-Cleaning Building Surface in an Urban Environment.” *Build. Environ.*, **147** 506–516. <https://doi.org/10.1016/j.buildenv.2018.10.037> (2019)
  73. Liu, N, Zhu, Q, Zhang, N, Zhang, C, Kawazoe, N, Chen, G, Negishi, N, Yang, Y, “Superior Disinfection Effect of *Escherichia coli* by Hydrothermal Synthesized TiO<sub>2</sub>-Based Composite Photocatalyst Under LED Irradiation: Influence of Environmental Factors and Disinfection Mechanism.” *Environ. Pollut.*, **247** 847–856. <https://doi.org/10.1016/j.envpol.2019.01.082> (2019)
  74. Wang, Y, Rao, L, Wang, P, Shi, Z, Zhang, L, “Photocatalytic Activity of N-TiO<sub>2</sub>/O-Doped N Vacancy g-C<sub>3</sub>N<sub>4</sub> and the Intermediates Toxicity Evaluation Under Tetracycline Hydrochloride and Cr(VI) Coexistence Environment.” *Appl. Catal. B Environ.*, **262** 118308. <https://doi.org/10.1016/j.apcatb.2019.118308> (2020)
  75. Zhang, J, Jiang, L, Wu, D, Yin, Y, Guo, H, “Effects of Environmental Factors on the Growth and Microcystin Production of *Microcystis aeruginosa* under TiO<sub>2</sub> Nanoparticles Stress.” *Sci. Total Environ.*, **734** 139443. <https://doi.org/10.1016/j.scitotenv.2020.139443> (2020)
  76. <https://www.scopus.com/results/results.uri?sort=plf-f&src=s&sid=d770fc3891ef4a2e87ef59489857d707&sot=a&sdt=a&sl=35&s=titanium+dioxide+paints+or+coatings&origin=searchadvanced&editSaveSearch=&txGid=68c5b0f21341a7439eb9c3258809aee1>, (n.d.)
  77. Khlyustova, A, Sirotkin, N, Kusova, T, Kraev, A, Titov, V, Agafonov, A, “Doped TiO<sub>2</sub>: The Effect of Doping Elements on Photocatalytic Activity.” *Mater. Adv.*, **1** 1193–1201. <https://doi.org/10.1039/D0MA00171F> (2020)
  78. Colpani, GL, Zanetti, M, Zeferino, RCF, Silva, LL, Muneron, JM, de Mello, H, Riella, G, Padoin, N, Fiori, MA, Soares, C, “Lanthanides Effects on TiO<sub>2</sub> Photocatalysts.” In: *Photocatalysts-Applications and Attributes*. IntechOpen. <https://doi.org/10.5772/intechopen.80906> (2019)
  79. Liao, C, Li, Y, Tjong, SC, “Visible-Light Active Titanium Dioxide Nanomaterials with Bactericidal Properties.” *Nanomaterials*, **10** 124. <https://doi.org/10.3390/nano10010124> (2020)
  80. Yu, J-H, Nam, S-H, Lee, JW, Kim, DI, Boo, J-H, “Oxidation State and Structural Studies of Vanadium-Doped Titania Particles for the Visible Light-Driven Photocatalytic Activity.” *Appl. Surf. Sci.*, **472** 46–53. <https://doi.org/10.1016/j.apsusc.2018.04.125> (2019)
  81. Wysocka, I, Kowalska, E, Ryl, J, Nowaczyk, G, Zielińska-Jurek, A, “Morphology, Photocatalytic and Antimicrobial Properties of TiO<sub>2</sub> Modified with Mono- and Bimetallic Copper Platinum and Silver Nanoparticles.” *Nanomaterials*, **9** 1129. <https://doi.org/10.3390/nano9081129> (2019)
  82. Liu, T, Chen, W, Liu, X, Zhu, J, Lu, L, “Well-Dispersed Ultrafine Nitrogen-Doped TiO<sub>2</sub> with Polyvinylpyrrolidone (PVP) Acted as N-Source and Stabilizer for Water Splitting.” *J. Energy Chem.*, **25** 1–9. <https://doi.org/10.1016/j.jecchem.2015.11.009> (2016)
  83. Ansari, SA, Khan, MM, Ansari, MO, Cho, MH, “Nitrogen-Doped Titanium Dioxide (N-doped TiO<sub>2</sub>) for Visible Light Photocatalysis.” *New J. Chem.*, **40** 3000–3009. <https://doi.org/10.1039/C5NJ03478G> (2016)
  84. Kwon, J, Choi, K, Schreck, M, Liu, T, Tervoort, E, Niederberger, M, “Gas-Phase Nitrogen Doping of Monolithic TiO<sub>2</sub> Nanoparticle-Based Aerogels for Efficient Visible Light-Driven Photocatalytic H<sub>2</sub> Production.” *ACS Appl. Mater. Interfaces*, **13** 53691–53701. <https://doi.org/10.1021/acsami.1c12579> (2021)
  85. Calisir, MD, Gungor, M, Demir, A, Kilic, A, Khan, MM, “Nitrogen-Doped TiO<sub>2</sub> Fibers for Visible-Light-Induced Photocatalytic Activities.” *Ceram. Int.*, **46** 16743–16753. <https://doi.org/10.1016/j.ceramint.2020.03.250> (2020)
  86. Du, S, Lian, J, Zhang, F, “Visible Light-Responsive N-Doped TiO<sub>2</sub> Photocatalysis: Synthesis, Characterizations, and Applications.” *Trans. Tianjin Univ.*, **28** 33–52. <https://doi.org/10.1007/s12209-021-00303-w> (2022)
  87. Umebayashi, T, Yamaki, T, Yamamoto, S, Miyashita, A, Tanaka, S, Sumita, T, Asai, K, “Sulfur-Doping of Rutile-Titanium Dioxide by Ion Implantation: Photocurrent Spectroscopy and First-Principles Band Calculation Studies.” *J. Appl. Phys.*, **93** 5156–5160. <https://doi.org/10.1063/1.1565693> (2003)
  88. Ohno, T, Akiyoshi, M, Umebayashi, T, Asai, K, Mitsui, T, Matsumura, M, “Preparation of S-Doped TiO<sub>2</sub> Photocatalysts and their Photocatalytic Activities Under Visible Light.” *Appl. Catal. A Gen.*, **265** 115–121. <https://doi.org/10.1016/j.apcata.2004.01.007> (2004)
  89. Yu, JC, Ho, W, Yu, J, Yip, H, Wong, PK, Zhao, J, “Efficient Visible-Light-Induced Photocatalytic Disinfection on Sulfur-Doped Nanocrystalline Titania.” *Environ. Sci. Technol.*, **39** 1175–1179. <https://doi.org/10.1021/es035374h> (2005)
  90. Ansari, SA, Cho, MH, “Highly Visible Light Responsive, Narrow Band Gap TiO<sub>2</sub> Nanoparticles Modified by Elemental Red Phosphorus for Photocatalysis and Photoelectrochemical Applications.” *Sci. Rep.*, **6** 25405. <https://doi.org/10.1038/srep25405> (2016)
  91. Uk Lee, H, Lee, SC, Won, J, Son, B-C, Choi, S, Kim, Y, Park, SY, Kim, H-S, Lee, Y-C, Lee, J, “Stable Semiconductor Black Phosphorus (BP)@Titanium Dioxide (TiO<sub>2</sub>) Hybrid Photocatalysts.” *Sci. Rep.*, **5** 8691. <https://doi.org/10.1038/srep08691> (2015)
  92. Piątkowska, A, Janus, M, Szymański, K, Mozia, S, “C-, N- and S-Doped TiO<sub>2</sub> Photocatalysts: A Review.” *Catalysts*, **11** 144. <https://doi.org/10.3390/catal11010144> (2021)
  93. Wang, X, Cao, L, Lu, F, Meziani, MJ, Li, H, Qi, G, Sun, YP, “Photoinduced Electron Transfers with Carbon Dots.”

- Chem. Commun.*, **25** 3774–3776. <https://doi.org/10.1039/b906252a> (2009)
94. Shen, S, Chen, K, Wang, H, Fu, J, “Construction of Carbon Dots-Deposited TiO<sub>2</sub> Photocatalysts with Visible-Light-Induced Photocatalytic Activity for the Elimination of Pollutants.” *Diam. Relat. Mater.*, **124** 108896. <https://doi.org/10.1016/j.diamond.2022.108896> (2022)
  95. Elkodous, MA, Hassaan, A, Pal K, Ghoneim, AI, Abdeen, Z, “C-dots Dispersed Macro-mesoporous TiO<sub>2</sub> Photocatalyst for Effective Waste Water Treatment.” *Charact. Appl. Nanomater.*, **1** (2) (2018). <https://doi.org/10.24294/can.v1i2.585>
  96. Miao, R, Luo, Z, Zhong, W, Chen, S-Y, Jiang, T, Dutta, B, Nasr, Y, Zhang, Y, Suib, SL, “Mesoporous TiO<sub>2</sub> Modified with Carbon Quantum Dots as a High-Performance Visible Light Photocatalyst.” *Appl. Catal. B Environ.*, **189** 26–38. <https://doi.org/10.1016/j.apcatb.2016.01.070> (2016)
  97. Saud, PS, Pant, B, Alam, A-M, Ghouri, ZK, Park, M, Kim, H-Y, “Carbon Quantum Dots Anchored TiO<sub>2</sub> Nanofibers: Effective Photocatalyst for Waste Water Treatment.” *Ceram. Int.*, **41** 11953–11959. <https://doi.org/10.1016/j.ceramint.2015.06.007> (2015)
  98. Yu, H, Zhao, Y, Zhou, C, Shang, L, Peng, Y, Cao, Y, Wu, L-Z, Tung, C-H, Zhang, T, “Carbon Quantum Dots/TiO<sub>2</sub> Composites for Efficient Photocatalytic Hydrogen Evolution.” *J. Mater. Chem. A.*, **2** 3344. <https://doi.org/10.1039/c3ta14108j> (2014)
  99. Bai, L, Liu, L, Pang, J, Chen, Z, Wei, M, Wu, Y, Dong, G, Zhang, J, Shan, D, Wang, B, “N, P-Codoped Carbon Quantum Dots-Decorated TiO<sub>2</sub> Nanowires as Nanosized Heterojunction Photocatalyst with Improved Photocatalytic Performance for Methyl Blue Degradation.” *Environ. Sci. Pollut. Res.*, **29** 9932–9943. <https://doi.org/10.1007/s11356-021-16295-y> (2022)
  100. Rahbar, M, Mehrzad, M, Behpour, M, Mohammadi-Aghdam, S, Ashrafi, M, “S, N Co-Doped Carbon Quantum Dots/TiO<sub>2</sub> Nanocomposite as Highly Efficient Visible Light Photocatalyst.” *Nanotechnology.*, **30** 505702. <https://doi.org/10.1088/1361-6528/ab40dc> (2019)
  101. Jain, A, Vaya, D, “Photocatalytic Activity Of TiO<sub>2</sub> Nanomaterial.” *J. Chil. Chem. Soc.*, **62** 3683–3690. <https://doi.org/10.4067/s0717-97072017000403683> (2017)
  102. Padmanabhan, NT, Thomas, N, Louis, J, Mathew, DT, Ganguly, P, John, H, Pillai, SC, “Graphene Coupled TiO<sub>2</sub> Photocatalysts for Environmental Applications: A Review.” *Chemosphere*, **271** 129506. <https://doi.org/10.1016/j.chemosphere.2020.129506> (2021)
  103. Ren, Y, Han, Q, Su, Q, Yang, J, Zhao, Y, Wen, H, Jiang, Z, “Effects of 4d Transition Metals Doping on the Photocatalytic Activities of Anatase TiO<sub>2</sub> (101) Surface.” *Int. J. Quantum Chem.*, **121** (16) e26683. <https://doi.org/10.1002/qua.26683> (2021)
  104. Jiang, L, He, J, Yang, Y, Mao, D, Chen, D, Wang, W, Chen, Y, Sharma, VK, Wang, J, “Enhancing Visible-Light Photocatalytic Activity of Hard-Biotemplated TiO<sub>2</sub>: From Macrostructural Morphology Replication to Microstructural Building Units Design.” *J. Alloys Compd.*, **898** 162886. <https://doi.org/10.1016/j.jallcom.2021.162886> (2022)
  105. Ma, S, Gu, J, Han, Y, Gao, Y, Zong, Y, Ye, Z, Xue, J, “Facile Fabrication of C-TiO<sub>2</sub> Nanocomposites with Enhanced Photocatalytic Activity for Degradation of Tetracycline.” *ACS Omega*, **4** 21063–21071. <https://doi.org/10.1021/acsomega.9b02411> (2019)
  106. Lee, J-H, Mun, S-J, Lee, S-Y, Park, S-J, “Promoted Charge Separation and Specific Surface Area via Interlacing of N-Doped Titanium Dioxide Nanotubes on Carbon Nitride Nanosheets for Photocatalytic Degradation of Rhodamine B.” *Nanotechnol. Rev.*, **11** 1592–1605. <https://doi.org/10.1515/ntrev-2022-0085> (2022)
  107. Lee, J-C, Gopalan, A-I, Saianand, G, Lee, K-P, Kim, W-J, “Manganese and Graphene Included Titanium Dioxide Composite Nanowires: Fabrication Characterization and Enhanced Photocatalytic Activities.” *Nanomaterials*, **10** 456. <https://doi.org/10.3390/nano10030456> (2020)
  108. Huang, J, Fu, K, Deng, X, Yao, N, Wei, M, “Fabrication of TiO<sub>2</sub> Nanosheet Aarrays/Graphene/Cu<sub>2</sub>O Composite Structure for Enhanced Photocatalytic Activities.” *Nanoscale Res. Lett.*, **12** 310. <https://doi.org/10.1186/s11671-017-2088-7> (2017)
  109. El Mragui, A, Logvina, Y, Pinto da Silva, L, Zegaoui, O, Esteves da Silva, JCG, “Synthesis of Fe-and Co-Doped TiO<sub>2</sub> with Improved Photocatalytic Activity Under Visible Irradiation Toward Carbamazepine Degradation.” *Materials*, **12** 3874. <https://doi.org/10.3390/ma12233874> (2019)
  110. Salomatina, EV, Fukina, DG, Koryagin, AV, Titaev, DN, Suleimanov, EV, Smirnova, LA, “Preparation and Photocatalytic Properties of Titanium Dioxide Modified with Gold or Silver Nanoparticles.” *J. Environ. Chem. Eng.*, **9** 106078. <https://doi.org/10.1016/j.jece.2021.106078> (2021)
  111. Zhang, H, Tang, Q, Li, Q, Song, Q, Wu, H, Mao, N, “Enhanced Photocatalytic Properties of PET Filaments Coated with Ag-N Co-Doped TiO<sub>2</sub> Nanoparticles Sensitized with Disperse Blue Dyes.” *Nanomaterials*, **10** 987. <https://doi.org/10.3390/nano10050987> (2020)
  112. Shetty, V, “Solar Light Active Biogenic Titanium Dioxide Embedded Silver Oxide (AgO/Ag<sub>2</sub>O@ TiO<sub>2</sub>) Nanocomposite Structures for Dye Degradation by Photocatalysis.” *Mater. Sci. Semicond. Process.*, **132** 105923. <https://doi.org/10.1016/j.mssp.2021.105923> (2021)
  113. Zhao, Z, Li, Z, Zou, Z, “Structure and Properties of Water on the Anatase TiO<sub>2</sub> (101) Surface: From Single-Molecule Adsorption to Interface Formation.” *J. Phys. Chem. C.*, **116** 11054–11061. <https://doi.org/10.1021/jp301468c> (2012)
  114. Chen, L, Tian, L, Xie, J, Zhang, C, Chen, J, Wang, Y, Li, Q, Lv, K, Deng, K, “One-Step Solid State Synthesis of Facet-Dependent Contact TiO<sub>2</sub> Hollow Nanocubes and Reduced Graphene Oxide Hybrids with 3D/2D Heterojunctions for Enhanced Visible Photocatalytic Activity.” *Appl. Surf. Sci.*, **504** 144353. <https://doi.org/10.1016/j.apsusc.2019.144353> (2020)
  115. Padmanabhan, NT, Jayaraj, MK, John, H, “Mechanistic Insights into CTAB Assisted TiO<sub>2</sub> Crystal Growth with Largely Exposed High Energy Crystal Facets.” *J. Environ. Chem. Eng.*, **6** 5510–5519. <https://doi.org/10.1016/j.jece.2018.08.045> (2018)
  116. Padmanabhan, NT, Thomas, RM, John, H, “Antibacterial Self-Cleaning Binary and Ternary Hybrid Photocatalysts of Titanium Dioxide with Silver and Graphene.” *J. Environ. Chem. Eng.*, **10** 107275. <https://doi.org/10.1016/j.jece.2022.107275> (2022)
  117. Alavi, M, Varma, RS, “Phytosynthesis and Modification of Metal and Metal Oxide Nanoparticles/Nanocomposites for Antibacterial and Anticancer Activities: Recent Advances.” *Sustain. Chem. Pharm.*, **21** 100412. <https://doi.org/10.1016/j.scp.2021.100412> (2021)
  118. Mathew, S, Ganguly, P, Rhatigan, S, Kumaravel, V, Byrne, C, Hinder, S, Bartlett, J, Nolan, M, Pillai, S, “Cu-Doped TiO<sub>2</sub>: Visible Light Assisted Photocatalytic Antimicrobial Activity.” *Appl. Sci.*, **8** 2067. <https://doi.org/10.3390/ap8112067> (2018)
  119. Endo, M, Wei, Z, Wang, K, Karabiyik, B, Yoshiiri, K, Rokicka, P, Ohtani, B, Markowska-Szczupak, A, Kowalska,

- E, “Noble Metal-Modified Titania with Visible-Light Activity for the Decomposition of Microorganisms.” *Beilstein J. Nanotechnol.*, **9** 829–841. <https://doi.org/10.3762/bjnano.9.77> (2018)
120. Alavi, M, Jabari, E, Jabbari, E, “Functionalized Carbon-Based Nanomaterials and Quantum Dots with Antibacterial Activity: A Review.” *Expert Rev. Anti. Infect. Ther.*, **19** 35–44. <https://doi.org/10.1080/14787210.2020.1810569> (2021)
  121. Yan, Y, Kuang, W, Shi, L, Ye, X, Yang, Y, Xie, X, Shi, Q, Tan, S, “Carbon Quantum Dot-Decorated TiO<sub>2</sub> for Fast and Sustainable Antibacterial Properties Under Visible-Light.” *J. Alloys Compd.*, **777** 234–243. <https://doi.org/10.1016/j.jallcom.2018.10.191> (2019)
  122. Kotzias, D, Binas, V, Kiriakidis, G, “Smart Surfaces: Photocatalytic Degradation of Priority Pollutants on TiO<sub>2</sub>-Based Coatings in Indoor and Outdoor Environments—Principles and Mechanisms.” *Materials*, **15** 402. <https://doi.org/10.3390/ma15020402> (2022)
  123. Liu, G, Xia, H, Niu, Y, Zhao, X, Zhang, G, Song, L, Chen, H, “Fabrication of Self-Cleaning Photocatalytic Durable Building Coating Based on WO<sub>3</sub>-TNs/PDMS and NO Degradation Performance.” *Chem. Eng. J.*, **409** 128187. <https://doi.org/10.1016/j.cej.2020.128187> (2021)
  124. Salvadores, F, Reli, M, Alfano, OM, Kočí, K, Ballari, MDLM, “Efficiencies Evaluation of Photocatalytic Paints Under Indoor and Outdoor Air Conditions.” *Front. Chem.*, **8** 551710. <https://doi.org/10.3389/fchem.2020.551710> (2020)
  125. Salvadores, F, Alfano, OM, Ballari, MM, “Kinetic Study of Air Treatment by Photocatalytic Paints Under Indoor Radiation Source: Influence of Ambient Conditions and Photocatalyst Content.” *Appl. Catal. B Environ.*, **268** 118694. <https://doi.org/10.1016/j.apcatb.2020.118694> (2020)
  126. Peeters, H, Keulemans, M, Nuyts, G, Vanmeert, F, Li, C, Minjauw, M, Detavernier, C, Bals, S, Lenaerts, S, Verbruggen, SW, “Plasmonic Gold-Embedded TiO<sub>2</sub> Thin Films as Photocatalytic Self-Cleaning Coatings.” *Appl. Catal. B Environ.*, **267** 118654. <https://doi.org/10.1016/j.apcatb.2020.118654> (2020)
  127. Moongraksathum, B, Chien, M-Y, Chen, Y-W, “Antiviral and Antibacterial Effects of Silver-Doped TiO<sub>2</sub> Prepared by the Peroxo Sol-Gel Method.” *J. Nanosci. Nanotechnol.*, **19** 7356–7362. <https://doi.org/10.1166/jnn.2019.16615> (2019)
  128. Bucuresteanu RC, Husch M, Ionita M, Raditoiu V, Chihaiia V, Marcu C, Ditu LM, Mihaescu G, “New Antimicrobial Strategie Using Compositions With Photocatalytic Properties.” In: *Proc. Conf. CIE 2021, International Commission on Illumination, CIE, 2021*: pp. 149–164. <https://doi.org/10.25039/x48.2021.OP17>
  129. Tahmasebizad, N, Hamedani, MT, Shaban Ghazani, M, Pazhuhhanfar, Y, “Photocatalytic Activity and Antibacterial Behavior of TiO<sub>2</sub> Coatings Co-Doped with Copper and Nitrogen via Sol-Gel Method.” *J. Sol-Gel Sci. Technol.*, **93** 570–578. <https://doi.org/10.1007/s10971-019-05085-1> (2020)
  130. De Falco, G, Ciardiello, R, Commodo, M, Del Gaudio, P, Minutolo, P, Porta, A, D’Anna, A, “TiO<sub>2</sub> Nanoparticle Coatings with Advanced Antibacterial and Hydrophilic Properties Prepared by Flame Aerosol Synthesis and Thermophoretic Deposition.” *Surf. Coat. Technol.*, **349** 830–837. <https://doi.org/10.1016/j.surfcoat.2018.06.083> (2018)
  131. Arango-Santander, S, Pelaez-Vargas, A, Freitas, SC, García, C, “A Novel Approach to Create An Antibacterial Surface Using Titanium Dioxide and a Combination of Dip-Pen Nanolithography and Soft Lithography.” *Sci. Rep.*, **8** 15818. <https://doi.org/10.1038/s41598-018-34198-w> (2018)
  132. Gao, J, Li, W, Zhao, X, Wang, L, Pan, N, “Durable Visible Light Self-Cleaning Surfaces Imparted by TiO<sub>2</sub>/SiO<sub>2</sub>/GO Photocatalyst.” *Text. Res. J.*, **89** 517–527. <https://doi.org/10.1177/0040517517750647> (2019)
  133. Ghows, N, Entezari, MH, “Ultrasound with Low Intensity Assisted the Synthesis of Nanocrystalline TiO<sub>2</sub> Without Calcination.” *Ultrason. Sonochem.*, **17** 878–883. <https://doi.org/10.1016/j.ultsonch.2010.03.010> (2010)
  134. Behzadnia, A, Montazer, M, Rashidi, A, Mahmoudi Rad, M, “Rapid Sonosynthesis of N-Doped Nano TiO<sub>2</sub> on Wool Fabric at Low Temperature: Introducing Self-cleaning, Hydrophilicity, Antibacterial/Antifungal Properties with Low Alkali Solubility, Yellowness and Cytotoxicity.” *Photochem. Photobiol.*, **90** 1224–1233. <https://doi.org/10.1111/php.12324> (2014)
  135. Stan, MS, Badea, MA, Pircalabioru, GG, Chifriuc, MC, Diamandescu, L, Dumitrescu, I, Trica, B, Lambert, C, Dinischiotu, A, “Designing Cotton Fibers Impregnated with Photocatalytic Graphene Oxide/Fe, N-Doped TiO<sub>2</sub> Particles as Prospective Industrial Self-Cleaning and Biocompatible Textiles.” *Mater. Sci. Eng. C.*, **94** 318–332. <https://doi.org/10.1016/j.msec.2018.09.046> (2019)
  136. Gapusan, RB, Balela, MDL, “Visible Light-Induced Photocatalytic and Antibacterial Activity of TiO<sub>2</sub>/Polyaniline-Kapok Fiber Nanocomposite.” *Polym. Bull.*, **79** 3891–3910. <https://doi.org/10.1007/s00289-021-03679-w> (2022)
  137. Souza, DC, Amorim, SM, Cadamuro, RD, Fongaro, G, Peralta, RA, Peralta, RM, Puma, GL, Moreira, RF, “Hydrophobic Cellulose-Based and Non-Woven Fabrics Coated with Mesoporous TiO<sub>2</sub> and Their Virucidal Properties Under Indoor Light.” *Carbohydr. Polym. Technol. Appl.*, **3** 100182. <https://doi.org/10.1016/j.carpta.2021.100182> (2022)
  138. Zhao, Y, Tao, C, Xiao, G, Su, H, “Controlled Synthesis and Wastewater Treatment of Ag<sub>2</sub>O/TiO<sub>2</sub> Modified Chitosan-Based Photocatalytic Film.” *RSC Adv.*, **7** 11211–11221. <https://doi.org/10.1039/C6RA27295A> (2017)
  139. Pakdel, E, Zhao, H, Wang, J, Tang, B, Varley, RJ, Wang, X, “Superhydrophobic and Photocatalytic Self-Cleaning Cotton Fabric Using Flower-like N-Doped TiO<sub>2</sub>/PDMS Coating.” *Cellulose*, **28** 8807–8820. <https://doi.org/10.1007/s10570-021-04075-3> (2021)
  140. Cai, T, Fang, G, Tian, X, Yin, J-J, Chen, C, Ge, C, “Optimization of Antibacterial Efficacy of Noble-Metal-Based Core-Shell Nanostructures and Effect of Natural Organic Matter.” *ACS Nano*, **13** 12694–12702. <https://doi.org/10.1021/acsnano.9b04366> (2019)
  141. Yeh, MY, Yang, TY, Wu, TC, Lee, SY, Chang, SH, “Visible-Light Photocatalytic Activity of Fe@TiO<sub>2</sub> Core-Shell Composite Synthesized by Sol-Gel Method.” *Int. J. Mod. Phys. B.*, **34** 2040127. <https://doi.org/10.1142/S021797922040127X> (2020)
  142. Ferreira, O, Monteiro, OC, do Rego, AMB, Ferraria, AM, Batista, M, Santos, R, Monteiro, S, Freire, M, Silva, ER, “Visible Light-Driven Photodegradation of Triclosan and Antimicrobial Activity Against *Legionella pneumophila* with Cobalt and Nitrogen Co-Doped TiO<sub>2</sub> Anatase Nanoparticles.” *J. Environ. Chem. Eng.*, **9** 106735. <https://doi.org/10.1016/j.jece.2021.106735> (2021)
  143. Liu, B, Li, J, Wu, Y, Han, X, Liu, S, Zhang, J, Shi, H, “Plasmonic Ag Supported on Ni-Doped TiO<sub>2</sub> Nanospheres for Rapid Microbial Inactivation Under Visible Light.” *J. Alloys Compd.*, **882** 160717. <https://doi.org/10.1016/j.jallcom.2021.160717> (2021)
  144. Mutalik, C, Hsiao, Y-C, Chang, Y-H, Krisnawati, DI, Alimansur, M, Jazidie, A, Nuh, M, Chang, C-C, Wang, D-

- Y, Kuo, T-R, “High UV-Vis-NIR Light-Induced Antibacterial Activity by Heterostructured TiO<sub>2</sub>-FeS<sub>2</sub> Nanocomposites.” *Int. J. Nanomedicine.*, **15** 8911–8920. <https://doi.org/10.2147/IJN.S282689> (2020)
145. Tzeng, J-H, Weng, C-H, Yen, L-T, Gaybullaev, G, Chang, C-J, de Luna, MDG, Lin, Y-T, “Inactivation of Pathogens by Visible Light Photocatalysis with Nitrogen-Doped TiO<sub>2</sub> and Tourmaline-Nitrogen Co-Doped TiO<sub>2</sub>.” *Sep. Purif. Technol.*, **274** 118979. <https://doi.org/10.1016/j.seppur.2021.118979> (2021)
  146. Cao, Y, Wu, R, Zhang, W, Luo, J, Li, Y, Ning, L, Shen, R, Wang, D, Ye, W, “Killing Two Birds with One Stone: Silver Nanoparticles Loaded on Ultrathin N-Doped Carbon-Coated TiO<sub>2</sub> Porous Spheres with Narrow Bandgap for Efficient SERS Sensing and Photoinduced Antibacterial Applications.” *Appl. Surf. Sci.*, **583** 152512. <https://doi.org/10.1016/j.apsusc.2022.152512> (2022)
  147. Ashfaq, A, Ikram, M, Haider, A, Ul-Hamid, A, Shahzadi, I, Haider, J, “Nitrogen and Carbon Nitride-Doped TiO<sub>2</sub> for Multiple Catalysis and Its Antimicrobial Activity.” *Nanoscale Res. Lett.*, **16** 119. <https://doi.org/10.1186/s11671-021-03573-4> (2021)
  148. Deshmukh, SP, Koli, VB, Dhodamani, AG, Patil, SM, Ghodake, VS, Delekar, SD, “Ultrasonochemically Modified Ag@TiO<sub>2</sub> Nanocomposites as Potent Antibacterial Agent in the Paint Formulation for Surface Disinfection.” *ChemistrySelect*, **6** 113–122. <https://doi.org/10.1002/slct.2020.02903> (2021)
  149. Bode-Aluko, CA, Pereao, O, Kyaw, HH, Al-Naamani, L, Al-Abri, MZ, Myint, MT, Rossouw, A, Fatoba, O, Petrik, L, Dobretsov, S, “Photocatalytic and Antifouling Properties of Electrospun TiO<sub>2</sub> Polyacrylonitrile Composite Nanofibers Under Visible Light.” *Mater. Sci. Eng. B.*, **1** (264) 114913. <https://doi.org/10.1016/j.mseb.2020.114913> (2021)
  150. Aravind, M, Amalanathan, M, Mary, MSM, Parvathiraja, C, Allothman, AA, Wabaidur, SM, Islam, MA, “Enhanced Photocatalytic and Biological Observations of Green Synthesized Activated Carbon, Activated Carbon Doped Silver and Activated Carbon/Silver/Titanium Dioxide Nanocomposites.” *J. Inorg. Organomet. Polym. Mater.*, **32** 267–279. <https://doi.org/10.1007/s10904-021-02096-w> (2022)
  151. Krumdieck, SP, Boichot, R, Gorthy, R, Land, JG, Lay, S, Gardecka, AJ, Polson, MIJ, Wasa, A, Aitken, JE, Heinemann, JA, Renou, G, Berthomé, G, Charlot, F, Encinas, T, Braccini, M, Bishop, CM, “Nanostructured TiO<sub>2</sub> Anatase-Rutile-Carbon Solid Coating with Visible Light Antimicrobial Activity.” *Sci. Rep.*, **9** 1883. <https://doi.org/10.1038/s41598-018-38291-y> (2019)
  152. Wasa, A, Land, JG, Gorthy, R, Krumdieck, S, Bishop, C, Godsoe, W, Heinemann, JA, “Antimicrobial and Biofilm-Disrupting Nanostructured TiO<sub>2</sub> Coating Demonstrating Photoactivity and Dark Activity.” *FEMS Microbiol. Lett.*, **368** fnab039. <https://doi.org/10.1093/femsle/fnab039> (2021)
  153. Park, GW, Cho, M, Cates, EL, Lee, D, Oh, B-T, Vinjé, J, Kim, J-H, “Fluorinated TiO<sub>2</sub> as an Ambient Light-Activated Virucidal Surface Coating Material for the Control of Human Norovirus.” *J. Photochem. Photobiol. B Biol.*, **140** 315–320. <https://doi.org/10.1016/j.jphotobiol.2014.08.009> (2014)
  154. Nagay, BE, Dini, C, Cordeiro, JM, Ricomini-Filho, AP, de Avila, ED, Rangel, EC, da Cruz, NC, Barão, VAR, “Visible-Light-Induced Photocatalytic and Antibacterial Activity of TiO<sub>2</sub> Codoped with Nitrogen and Bismuth: New Perspectives to Control Implant-Biofilm-Related Diseases.” *ACS Appl. Mater. Interfaces*, **11** 18186–18202. <https://doi.org/10.1021/acsami.9b03311> (2019)
  155. Zhang, Q, Ma, L, Shao, M, Huang, J, Ding, M, Deng, X, Wei, X, Xu, X, “Anodic Oxidation Synthesis of One-Dimensional TiO<sub>2</sub> Nanostructures for Photocatalytic and Field Emission Properties.” *J. Nanomater.*, **2014** 1–14. <https://doi.org/10.1155/2014/831752> (2014)
  156. Motola, M, Dworniczek, E, Satrapinsky, L, Chodaczek, G, Grzesiak, J, Gregor, M, Plecenik, T, Nowicka, J, Plesch, G, “UV Light-Induced Photocatalytic, Antimicrobial, and Antibiofilm Performance of Anodic TiO<sub>2</sub> Nanotube Layers Prepared on Titanium Mesh and Ti Sputtered on Silicon.” *Chem. Pap.*, **73** 1163–1172. <https://doi.org/10.1007/s11696-018-0667-4> (2019)
  157. Liu, J, Zhu, Y, Chen, J, Butenko, DS, Ren, J, Yang, X, Lu, P, Meng, P, Xu, Y, Yang, D, Zhang, S, “Visible-Light Driven Rapid Bacterial Inactivation on Red Phosphorus/Titanium Oxide Nanofiber Heterostructures.” *J. Hazard. Mater.*, **413** 125462. <https://doi.org/10.1016/j.jhazmat.2021.125462> (2021)
  158. Song, K, Cui, Y, Liu, L, Chen, B, Hirose, K, Shahiduzzaman, M, Umezu, S, “Electro-Spray Deposited TiO<sub>2</sub> Bilayer Films and Their Recyclable Photocatalytic Self-Cleaning Strategy.” *Sci. Rep.*, **12** 1582. <https://doi.org/10.1038/s41598-022-05633-w> (2022)
  159. Chanklom, P, Kreetachat, T, Chotigawin, R, Suwannahong, K, “Photocatalytic Oxidation of PLA/TiO<sub>2</sub>-Composite Films for Indoor Air Purification.” *ACS Omega*, **6** 10629–10636. <https://doi.org/10.1021/acsomega.0c06194> (2021)
  160. Solano, R, Patiño-Ruiz, D, Herrera, A, “Preparation of Modified Paints with Nano-Structured Additives and Its Potential Applications.” *Nanomater. Nanotechnol.*, **10** 184798042090918. <https://doi.org/10.1177/1847980420909188> (2020)
  161. Roopan, SM, Bharathi, A, Prabhakarn, A, Abdul Rahman, A, Velayutham, K, Rajakumar, G, Padmaja, RD, Lekshmi, M, Madhumitha, G, “Efficient Phyto-synthesis and Structural Characterization of Rutile TiO<sub>2</sub> Nanoparticles Using *Annona squamosa* Peel Extract.” *Spectrochim. Acta Part A Mol. Biomol. Spectrosc.*, **98** 86–90. <https://doi.org/10.1016/j.saa.2012.08.055> (2012)
  162. Vembu, S, Vijayakumar, S, Nilavukkarasi, M, Vidhya, E, Punitha, VN, “Phytosynthesis of TiO<sub>2</sub> Nanoparticles in Diverse Applications: What is the Exact Mechanism of Action?” *Sensors Int.*, **3** 100161. <https://doi.org/10.1016/j.sintl.2022.100161> (2022)
  163. Rajeshkumar, S, Santhoshkumar, J, Jule, LT, Ramaswamy, K, “Phytosynthesis of Titanium Dioxide Nanoparticles Using King of Bitter *Andrographis paniculata* and Its Embryonic Toxicology Evaluation and Biomedical Potential.” *Bioinorg. Chem. Appl.*, **2021** 1–11. <https://doi.org/10.1155/2021/6267634> (2021)
  164. Thakur, BK, Kumar, A, Kumar, D, “Green Synthesis of Titanium Dioxide Nanoparticles using *Azadirachta indica* Leaf Extract and Evaluation of Their Antibacterial Activity.” *South African J. Bot.*, **124** 223–227. <https://doi.org/10.1016/j.sajb.2019.05.024> (2019)
  165. Senthilkumar, S, Ashok, M, Kashinath, L, Sanjeeviraja, C, Rajendran, A, “Phytosynthesis and Characterization of TiO<sub>2</sub> Nanoparticles using *Diospyros ebenum* Leaf Extract and Their Antibacterial and Photocatalytic Degradation of Crystal Violet.” *Smart Sci.*, **6** 1–9. <https://doi.org/10.1080/23080477.2017.1410012> (2018)
  166. Akinola, PO, Lateef, A, Asafa, TB, Beukes, LS, Hakeem, AS, Irshad, HM, “Multifunctional Titanium Dioxide Nanoparticles Biofabricated via Phytosynthetic Route Using Extracts of *Cola nitida*: Antimicrobial, Dye Degradation, Antioxidant and Anticoagulant Activities.” *Heli-*

- yon, 6 e04610. <https://doi.org/10.1016/j.heliyon.2020.e04610> (2020)
167. Mahboob, S, Nivetha, R, Gopinath, K, Balalakshmi, C, Al-Ghanim, KA, Al-Misned, F, Ahmed, Z, Govindarajan, M, “Facile Synthesis of Gold and Platinum Doped Titanium Oxide Nanoparticles for Antibacterial and Photocatalytic Activity: A Photodynamic Approach.” *Photodiagnosis Photodyn. Ther.*, 33 102148. <https://doi.org/10.1016/j.pdpdt.2020.102148> (2021)
168. EL-Hefnawy ME, “Biodegradable Films from Phytosynthesized TiO<sub>2</sub> Nanoparticles and Nanofungal Chitosan as Probable Nanofertilizers.” *Int. J. Polym. Sci.*, 2020 1–7. <https://doi.org/10.1155/2020/6727132> (2020)
169. Sathishkumar, G, Aarthi, M, Senthilkumar, R, Nithiya, P, Selvakumar, R, Bhattacharyya, A, “Biodegradable Cellulosic Sanitary Napkins from Waste Cotton and Natural

Extract Based Anti-bacterial Nanocolorants.” *J. Indian Inst. Sci.*, 99 519–528. <https://doi.org/10.1007/s41745-019-00123-x> (2019)

**Publisher’s Note** Springer Nature remains neutral with regard to jurisdictional claims in published maps and institutional affiliations.

Springer Nature or its licensor (e.g. a society or other partner) holds exclusive rights to this article under a publishing agreement with the author(s) or other rightsholder(s); author self-archiving of the accepted manuscript version of this article is solely governed by the terms of such publishing agreement and applicable law.